Article

Not peer-reviewed version

Geometrized Vacuum Physics. Part III. Curved Vacuum Area

Mikhail Batanov-Gaukhman *

Posted Date: 5 October 2023

doi: 10.20944/preprints202308.0570.v4

Keywords: vacuum; vacuum layers; acceleration of vacuum layer; vacuum layer dynamics; vacuum electrostatics; rotation of nucleus

Article

Geometrized Vacuum Physics. Part III. Curved Vacuum Area

Mikhail Batanov-Gaukhman

Moscow Aviation Institute (National Research University), Institute No. 2 "Aircraft and rocket engines and power plants", st. Volokolamsk highway, 4, Moscow – Russia, 125993; alsignat@yandex.ru

Abstract: This article is the third part of a scientific project under the general title "Geometrized vacuum physics based on the Algebra of Signatures". In the first two papers [1,2], the ideal (i.e., non-curved and immobile) local region of vacuum was studied and the foundations of the Algebra of Signatures were laid. This article considers the possibilities of describing the curved and moving state of the same vacuum region on the basis of the mathematical apparatus of the Algebra of Signatures. The reasons for the multilateral consideration of vacuum and twisting of intra-vacuum processes into spiral bundles are disclosed. The 4-tensor is introduced for two-sided and 16-sided consideration of the curvature of the local vacuum region. On the basis of kinematic models, the following assumptions were made: about the inert properties of vacuum layers; about the possibility of displacement of vacuum layers relative to each other at a speed significantly exceeding the speed of light; about the possibility of "rupture" of the local region of vacuum. The proposed kinematic models of the movement of vacuum layers can be a theoretical basis for the development of "zero" (i.e., vacuum) technologies.

Keywords: vacuum; geometrized vacuum physics; signature; algebra of signature; vacuum distortion; curved vacuum

---

1. Background and Introduction

This work is the third of a series of articles under the title "Geometric vacuum physics". In the previous two articles [1,2], the foundations of the Algebra of Stignatures and the Algebra of Signatures were presented, which were obtained on the basis of the study of an ideal (i.e., non-curved and immobile) region of the vacuum.

This article considers the possibility of expanding the capabilities of the Algebra of Signatures to describe the curvature of the same region of the vacuum.

In §1 of the article [1], it was shown that as a result of probing an ideal region of vacuum with light rays with a wavelength $\lambda_{m,n}$ (from the subrange $\Delta\lambda = 10^m \div 10^n$ cm) from three mutually perpendicular directions makes it possible to obtain a light cubic lattice (see Figure 1 of the article [1]). Such a lattice illuminated from the void was called the $\lambda_{m,n}$-vacuum (or $3D_{m,n}$-landscape).

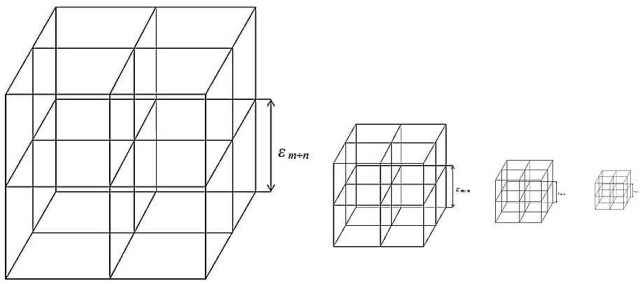

Figure 1. Discrete set of nested $\lambda_{m,n}$-vacuums of the same 3-dimensional volume of a vacuum, where $\lambda_{m,n} > \lambda_{m+1,n+1} > \lambda_{m+2,n+2} > \lambda_{m+3,n+3}$.

It was also shown in [1] that if we similarly probe the area of ideal vacuum with light rays of other wavelengths, we will obtain an infinite number of $\lambda_{m,n}$-vacuums (i.e., $3D_{m,n}$-landscapes with an

Preprints (www.preprints.org) | NOT PEER-REVIEWED | Posted: 5 October 2023 doi:10.20944/preprints202308.0570.v4

edge length cubic cell $\varepsilon_{m,n} \sim 100\lambda_{m,n}$) which nested into each other like nesting dolls (see Figure 1, or Figure 2 in [1]).

As already noted in §2 of the article [1], if the area of vacuum under study is not curved, then all $\lambda_{m,n}$-vacuums will be represented as ideal cubic $3D_{m,n}$-lattices, which differ from each other only by the length of the edge of cubic cell $\varepsilon_{m,n} \sim 10^2\lambda_{m,n}$ (see Figure 1).

However, if the region of vacuum under study is curved, then all $\lambda_{m,n}$-vacuums will differ somewhat from each other due to the fact that light rays (i.e., eikonals) with different wavelengths have different thicknesses (i.e., circular cross section of the eikonal, see Figure 2, or Figure 3 in [1]), which leads to averaging of vacuum curvature within the beam thickness.

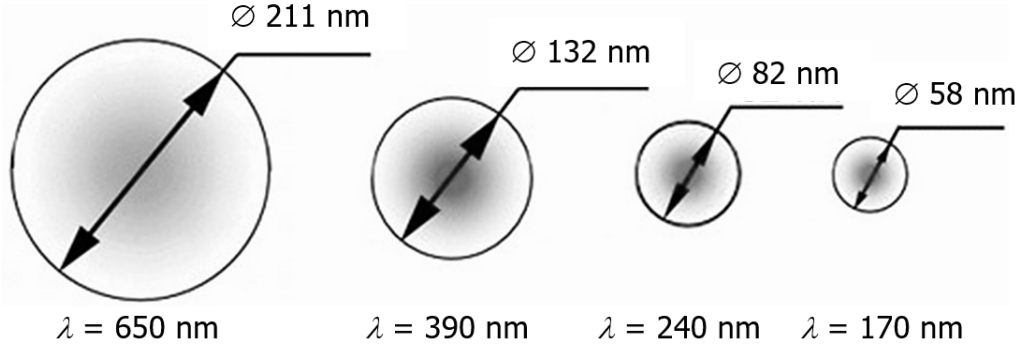

Figure 2. Experimental data on the thickness of the laser beam depending on the length wave λ of the corresponding monochromatic electromagnetic radiation.

In this case, each $\lambda_{m,n}$-vacuum (i.e., the light $3D_{m,n}$-landscape) will be unique. That is, each $\lambda_{m,n}$-vacuum is only one 3-dimensional "slice" of the curved vacuum region. For a complete description of a curved region of vacuum, it is necessary to have an infinite set of curved $\lambda_{m,n}$-vacuums nested in each other (see Figure 3 or Figure 4 in [1]).

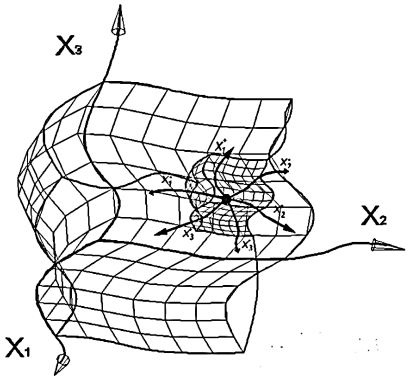

Figure 3. Illustration of a curved $\lambda_{m,n}$-vacuum embedded in curved $\lambda_{f,d}$-vacuum (where $\lambda_{f,d} > \lambda_{m,n}$).

Thus, the local volume of a curved area of vacuum is an infinitely complex system consisting of an infinite number of $\lambda_{m,n}$-vacuums nested in each other.

However, the situation is simplified by the fact that in the entire studied range of electromagnetic wave lengths, all $\lambda_{m,n}$-vacuums obey the same physical and geometric laws. Therefore, the method of describing one curved area of the $\lambda_{k,r}$-vacuum is automatically extended to all other $\lambda_{m,n}$-vacuums.

The mathematical apparatus of the Algebra of Stignatures is developed below, designed to study the local volume of only one curved $\lambda_{m,n}$-vacuum. But this mathematical apparatus is suitable for studying not only all $\lambda_{m,n}$-vacuums, but also any other deformed continuous media in which wave disturbances propagate at a constant speed.

Below, we develop the mathematical apparatus of the Algebra of Stignatures, designed to study the local volume of only one curved $\lambda_{m,n}$-vacuum. But this mathematical apparatus is suitable for

Preprints (www.preprints.org) | NOT PEER-REVIEWED | Posted: 5 October 2023 doi:10.20944/preprints202308.0570.v4

studying not only all $\lambda_{m,n}$-vacuums, but also any other deformed continuous media in which wave disturbances propagate at a constant speed.

2. Materials and Method

2.1. Curved area of $\lambda_{m,n}$-vacuum

Let's consider a curved area of vacuum. If the wavelength $\lambda_{m,n}$ of test monochromatic light rays is much smaller than the dimensions of the vacuum curvature, then in this area the cubic cell of the $\lambda_{m,n}$-vacuum (i.e., the cubic cell of the 3D$_{m,n}$-landscape, which limited by these rays) will be curved (see Figure 4*a*).

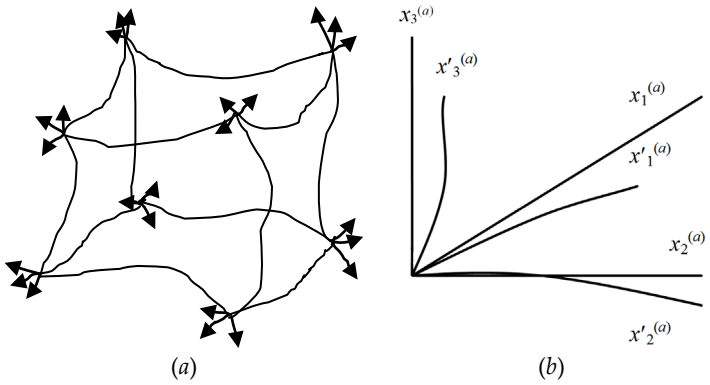

Figure 4. *a*) Curved cubic cell of the $\lambda_{m,n}$-vacuum; *b*) One of the corners of a curved $\lambda_{m,n}$-vacuum cubic cell.

We consider one of the eight vertices of the curved cube of the $\lambda_{m,n}$-vacuum (see Figure 4*a*). Let's replace the distorted edges emerging from this vertex with distorted axes of the curvilinear coordinate system $x'^{0(a)}$, $x'^{1(a)}$, $x'^{2(a)}$, $x^{3'(a)}$ (see Figure 4*b*). We denote the same edges of the original, ideal cube by the pseudo-Cartesian coordinate system $x^{0(a)}$, $x^{1(a)}$, $x^{2(a)}$, $x^{3(a)}$.

In the area of the vertex of the angle under consideration (see Figure 4*b*), its distortions can be decomposed into two components: 1) changing the lengths (compression or expansion) of the axes $x'^{0(a)}$, $x'^{1(a)}$, $x'^{2(a)}$, $x^{3'(a)}$ while maintaining right angles between these axes; 2) deviations of the angles between the axes $x'^{0(a)}$, $x'^{1(a)}$, $x'^{2(a)}$, $x'^{3(a)}$ from right angles (i.e., 90°) while preserving their lengths.

Let's consider these distortions separately.

1) Let only the lengths of the axes $x'^{0(a)}$, $x'^{1(a)}$, $x'^{2(a)}$, $x^{3'(a)}$ change near the vertex during the curvature, then these axes can be expressed through the original (ideal) axes $x^{0(a)}$, $x^{1(a)}$, $x^{2(a)}$, $x^{3(a)}$ using the corresponding coordinate transformations [3]:

$$\begin{aligned} x'^{0(a)} &= \alpha_{00}{}^{(a)}x^{0(a)} + \alpha_{01}{}^{(a)}x^{1(a)} + \alpha_{02}{}^{(a)}x^{2(a)} + \alpha_{03}{}^{(a)}x^{3(a)};\\ x'^{1(a)} &= \alpha_{10}{}^{(a)}x^{0(a)} + \alpha_{11}{}^{(a)}x^{1(a)} + \alpha_{12}{}^{(a)}x^{2(a)} + \alpha_{13}{}^{(a)}x^{3(a)};\\ x'^{2(a)} &= \alpha_{20}{}^{(a)}x^{0(a)} + \alpha_{21}{}^{(a)}x^{1(a)} + \alpha_{22}{}^{(a)}x^{2(a)} + \alpha_{23}{}^{(a)}x^{3(a)};\\ x'^{3\,(a)} &= \alpha_{30}{}^{(a)}x^{0(a)} + \alpha_{31}{}^{(a)}x^{1(a)} + \alpha_{32}{}^{(a)}x^{2(a)} + \alpha_{33}{}^{(a)}x^{3(a)}, \end{aligned} \tag{1}$$

where

$$\alpha_{ij}{}^{(a)} = dx'^{i(a)}/dx^{j(a)} \tag{2}$$

is the Jacobian of the transformation, or the components of the elongation tensor.

2) Now let the distortion near the vertex be associated only with a change in the angles between the axes of the coordinate system $x'^{0(a)}$, $x'^{1(a)}$, $x'^{2(a)}$, $x^{3'(a)}$, while the lengths of these axes remain unchanged. In this case, it is sufficient to consider only the change in the angles between the basis vectors $\mathbf{e}'_0{}^{(a)}$, $\mathbf{e}'_1{}^{(a)}$, $\mathbf{e}'_2{}^{(a)}$, $\mathbf{e}'_3{}^{(a)}$ of the distorted reference system.

Preprints (www.preprints.org) | NOT PEER-REVIEWED | Posted: 5 October 2023 doi:10.20944/preprints202308.0570.v4

It is known from vector analysis that the basis vectors of the distorted 4-basis $\mathbf{e'}_{0}{}^{(a)}$, $\mathbf{e'}_{1}{}^{(a)}$, $\mathbf{e'}_{2}{}^{(a)}$, $\mathbf{e'}_{3}{}^{(a)}$ can be expressed in terms of the original basis vectors $\mathbf{e}_{0}{}^{(a)}$, $\mathbf{e}_{1}{}^{(a)}$, $\mathbf{e}_{2}{}^{(a)}$, $\mathbf{e}_{3}{}^{(a)}$ of an orthogonal 4-basis by means of the following system of the linear equations [3]:

$$\begin{aligned}
\mathbf{e'}_{0}{}^{(a)} &= \beta^{00(a)}\,\mathbf{e}_{0}{}^{(a)} + \beta^{01(a)}\,\mathbf{e}_{1}{}^{(a)} + \beta^{02(a)}\,\mathbf{e}_{2}{}^{(a)} + \beta^{03(a)}\,\mathbf{e}_{3}{}^{(a)};\\
\mathbf{e'}_{1}{}^{(a)} &= \beta^{10(a)}\,\mathbf{e}_{0}{}^{(a)} + \beta^{11(a)}\,\mathbf{e}_{1}{}^{(a)} + \beta^{12(a)}\,\mathbf{e}_{2}{}^{(a)} + \beta^{13(a)}\,\mathbf{e}_{3}{}^{(a)};\\
\mathbf{e'}_{2}{}^{(a)} &= \beta^{20(a)}\,\mathbf{e}_{0}{}^{(a)} + \beta^{21(a)}\,\mathbf{e}_{1}{}^{(a)} + \beta^{22(a)}\,\mathbf{e}_{2}{}^{(a)} + \beta^{23(a)}\,\mathbf{e}_{3}{}^{(a)};\\
\mathbf{e'}_{3}{}^{(a)} &= \beta^{30(a)}\,\mathbf{e}_{0}{}^{(a)} + \beta^{31(a)}\,\mathbf{e}_{1}{}^{(a)} + \beta^{32(a)}\,\mathbf{e}_{2}{}^{(a)} + \beta^{03(a)}\,\mathbf{e}_{3}{}^{(a)},
\end{aligned} \tag{3}$$

where

$$\beta^{pm(a)} = (\mathbf{e'}_{p}{}^{(a)} \cdot \mathbf{e}_{m}{}^{(a)}) = \cos\,(\mathbf{e'}_{p}{}^{(a)} \,\hat{}\, \mathbf{e}_{m}{}^{(a)}) \tag{4}$$

are the guiding cosines.

The systems of Eqs. (1) and (3) can be represented in a compact form:

$$x'^{i\,(a)} = \alpha_{ij}{}^{(a)}\, x^{\,j(a)}, \tag{5}$$

$$\mathbf{e'}_{p}{}^{(a)} = \beta^{\,pm(a)}\,\mathbf{e}_{m}{}^{(a)}. \tag{6}$$

here and below, the "Einstein summation rule" is used.

For example, we write the vector (48) in [1]

$$d\mathbf{s}'^{(7)} = \mathbf{e}'_{i}{}^{(7)} dx'^{\,i\,(7)}. \tag{7}$$

in the distorted 4-basis, taking into account Exs. (5) and (6), vector (7) can be represented as

$$d\mathbf{s}'^{(7)} = \beta^{\,pm(7)}\,\mathbf{e}_{m}{}^{(7)} \alpha_{pj}{}^{(7)} dx^{j(7)}. \tag{8}$$

Distortions of the remaining 7 trihedral angles of the curved cube of the $\lambda_{m,n}$-vacuum (Figure 4) (i.e., the fifteen remaining 4-bases shown in Figure 5, or Figure 7 in [1]) are described in a similar way.

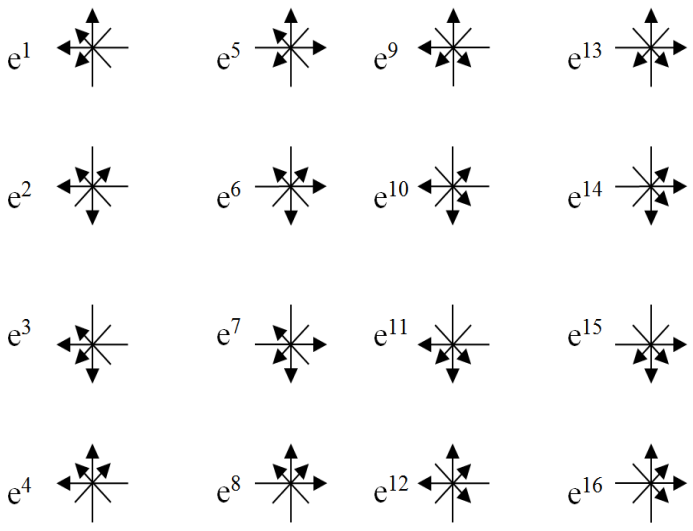

Figure 5. Sixteen 4-bases associated with eight corners of the $\lambda_{m,n}$-vacuum cube (repeat of the Figure 7 in [1]).

Thus, all sixteen 4-bases (see Figure 5) associated with the distorted trihedral angles of the $\lambda_{m,n}$-vacuum cube (see Figure 4) can be represented by the vectors

$$d\mathbf{s}'^{(a)} = \beta^{\,pm(a)}\,\mathbf{e}_{m}{}^{(a)}\,\alpha_{pj}{}^{(a)} dx^{j(a)}, \tag{9}$$

where $a = 1,2,\ldots,16$.

Preprints (www.preprints.org) | NOT PEER-REVIEWED | Posted: 5 October 2023 doi:10.20944/preprints202308.0570.v4

2.2. Curved metric 4-spaces

Consider two vectors (48) and (49) in [1], given in the 5th and 7th curved affine spaces

$$d\mathbf{s}'^{(5)} = \beta^{ln(5)}\mathbf{e}_n{}^{(5)}\alpha_{lj}{}^{(5)}dx^j, \tag{10}$$

$$d\mathbf{s}'^{(7)} = \beta^{pm(7)}\mathbf{e}_m{}^{(7)}\alpha_{pi}{}^{(7)}dx^i. \tag{11}$$

Let's find the scalar product of these vectors

$$ds'^{(7,5)2} = d\mathbf{s}'^{(7)}d\mathbf{s}'^{(5)} = \beta^{pm(7)}\mathbf{e}_m{}^{(7)}\alpha_{pi}{}^{(7)}\beta^{ln(5)}\mathbf{e}_n{}^{(5)}\alpha_{lj}{}^{(5)}dx^i dx^j = c_{ij}{}^{(7,5)}dx^i dx^j, \tag{12}$$

where

$$c_{ij}{}^{(7,5)} = \beta^{pm(7)}\mathbf{e}_m{}^{(7)}\alpha_{pi}{}^{(7)}\beta^{ln(5)}\mathbf{e}_n{}^{(5)}\alpha_{lj}{}^{(5)} \tag{13}$$

are the components of the metric tensor of the (7,5)-th metric 4-space.

Thus, we have obtained the metric of the (7,5)-th metric 4-space

$$ds'^{(7,5)2} = c_{ij}{}^{(7,5)}dx^i dx^j \tag{14}$$

with signature (53) in [1] (+ + + –) and metric tensor

$$c_{ij}^{(7,5)} = \begin{pmatrix} c_{00}^{(7,5)} & c_{10}^{(7,5)} & c_{20}^{(7,5)} & c_{30}^{(7,5)} \\ c_{01}^{(7,5)} & c_{11}^{(7,5)} & c_{21}^{(7,5)} & c_{31}^{(7,5)} \\ c_{02}^{(7,5)} & c_{12}^{(7,5)} & c_{22}^{(7,5)} & c_{32}^{(7,5)} \\ c_{03}^{(7,5)} & c_{13}^{(7,5)} & c_{23}^{(7,5)} & c_{33}^{(7,5)} \end{pmatrix}. \tag{15}$$

Similarly, the scalar pairwise product of any two of the 16 vectors (9)

$$d\mathbf{s}'^{(a)} = \beta^{pm(a)}\mathbf{e}_m{}^{(a)}\alpha_{pi}{}^{(a)}dx^i, \tag{16}$$

$$d\mathbf{s}'^{(b)} = \beta^{ln(b)}\mathbf{e}_n{}^{(b)}\alpha_{lj}{}^{(b)}dx^j \tag{17}$$

leads to the formation of an atlas consisting of 16 × 16 = 256 possible curved 4-sheets (that is, metric 4-spaces) with metrics

$$ds'^{(a,b)2} = c_{ij}{}^{(a,b)}dx^i dx^j, \tag{18}$$

where a = 1,2,3,…,16; b = 1,2,3,…,16, with corresponding signatures (11) in [2] and metric tensors

$$c_{ij}^{(a,b)} = \begin{pmatrix} c_{00}^{(a,b)} & c_{10}^{(a,b)} & c_{20}^{(a,b)} & c_{30}^{(a,b)} \\ c_{01}^{(a,b)} & c_{11}^{(a,b)} & c_{21}^{(a,b)} & c_{31}^{(a,b)} \\ c_{02}^{(a,b)} & c_{12}^{(a,b)} & c_{22}^{(a,b)} & c_{32}^{(a,b)} \\ c_{03}^{(a,b)} & c_{13}^{(a,b)} & c_{23}^{(a,b)} & c_{33}^{(a,b)} \end{pmatrix}, \tag{19}$$

where

$$c_{ij}{}^{(a,b)} = \beta^{pm(a)}\mathbf{e}_m{}^{(a)}\alpha_{pi}{}^{(a)}\beta^{ln(b)}\mathbf{e}_n{}^{(b)}\alpha_{lj}{}^{(b)} \tag{20}$$

are the components of the metric tensor of the (a,b)-th curved metric 4-space.

2.3. The first stage of compactification of curved measurements

Just as it was done in §2.3 in [2], at the first stage of the compactification of additional curved mathematical dimensions in the Algebra of Signatures, metric 4-spaces with the same signature are averaged.

For example, for metrics with signature (– + – +), we have the following averaged metric tensor

Preprints (www.preprints.org) | NOT PEER-REVIEWED | Posted: 5 October 2023 doi:10.20944/preprints202308.0570.v4

$$c_{ij}^{(p)} = \begin{pmatrix} c_{00}^{(p)} & c_{10}^{(p)} & c_{20}^{(p)} & c_{30}^{(p)} \\ c_{01}^{(p)} & c_{11}^{(p)} & c_{21}^{(p)} & c_{31}^{(p)} \\ c_{02}^{(p)} & c_{12}^{(p)} & c_{22}^{(p)} & c_{32}^{(p)} \\ c_{03}^{(p)} & c_{13}^{(p)} & c_{23}^{(p)} & c_{33}^{(p)} \end{pmatrix} = \frac{1}{16}\left\{ \begin{pmatrix} c_{00}^{(14,2)} & c_{10}^{(14,2)} & c_{20}^{(14,2)} & c_{30}^{(14,2)} \\ c_{01}^{(14,2)} & c_{11}^{(14,2)} & c_{21}^{(14,2)} & c_{31}^{(14,2)} \\ c_{02}^{(14,2)} & c_{12}^{(14,2)} & c_{22}^{(14,2)} & c_{32}^{(14,2)} \\ c_{03}^{(14,2)} & c_{13}^{(14,2)} & c_{23}^{(14,2)} & c_{33}^{(14,2)} \end{pmatrix} + \right.$$

$$+ \begin{pmatrix} c_{00}^{(13,1)} & c_{10}^{(13,1)} & c_{20}^{(13,1)} & c_{30}^{(13,1)} \\ c_{01}^{(13,1)} & c_{11}^{(13,1)} & c_{21}^{(13,1)} & c_{31}^{(13,1)} \\ c_{02}^{(13,1)} & c_{12}^{(13,1)} & c_{22}^{(13,1)} & c_{32}^{(13,1)} \\ c_{03}^{(13,1)} & c_{13}^{(13,1)} & c_{23}^{(13,1)} & c_{33}^{(13,1)} \end{pmatrix} + \left. \right\}, \tag{21}$$

$$\cdots\cdots\cdots\cdots\cdots\cdots\cdots\cdots\cdots\cdots$$

$$+ \begin{pmatrix} c_{00}^{(1,13)} & c_{10}^{(1,13)} & c_{20}^{(1,13)} & c_{30}^{(1,13)} \\ c_{01}^{(1,13)} & c_{11}^{(1,13)} & c_{21}^{(1,13)} & c_{31}^{(1,13)} \\ c_{02}^{(1,13)} & c_{12}^{(1,13)} & c_{22}^{(1,13)} & c_{32}^{(1,13)} \\ c_{03}^{(1,13)} & c_{13}^{(1,13)} & c_{23}^{(1,13)} & c_{33}^{(1,13)} \end{pmatrix} \Bigg\}$$

where p corresponds to the 14-th signature $(-+-+)$, according to the following conditional numbering of signatures:

$$sign\left(c_{ij}^{(p)}\right) = \begin{matrix} (+++)^1 & (+++-)^5 & (-++-)^9 & (++-+)^{13} \\ (---+)^2 & (-+++)^6 & (--++)^{10} & (-+-+)^{14} \\ (+--+)^3 & (++--)^7 & (+---)^{11} & (+-++)^{15} \\ (--+-)^4 & (+-+-)^8 & (-+--)^{12} & (----)^{16}. \end{matrix} \tag{22}$$

This matrix with numbered signatures corresponds to the matrix of signatures (32) in [2].

As a result of operation (21), the averaged metric is obtained

$$\langle ds^{(-+-+)2} \rangle = c_{ij}^{(14)} dx^i dx^j, \text{ with signature } (-+-+). \tag{23}$$

Similarly, as a result of averaging type (21) – (23) out of 256 metrics (18) of curved metric 4-spaces, we can obtain 256 : 16 = 16 averaged metrics with 16 possible signatures

$$\begin{matrix} \langle ds^{(+---)2} \rangle & \langle ds^{(++++)2} \rangle & \langle ds^{(---+)2} \rangle & \langle ds^{(+--+)2} \rangle \\ \langle ds^{(--+-)2} \rangle & \langle ds^{(++--)2} \rangle & \langle ds^{(-+--)2} \rangle & \langle ds^{(+-+-)2} \rangle \\ \langle ds^{(-+++)2} \rangle & \langle ds^{(----)2} \rangle & \langle ds^{(+++-)2} \rangle & \langle ds^{(-++-)2} \rangle \\ \langle ds^{(++-+)2} \rangle & \langle ds^{(--++)2} \rangle & \langle ds^{(+-++)2} \rangle & \langle ds^{(-+-+)2} \rangle, \end{matrix} \tag{24}$$

where ‹ › means averaging.

If the additive superposition (i.e., summation) of all these 16 averaged metrics (24) is equal to zero

$$ds_\Sigma^2 = \frac{1}{16}\sum_{p=1}^{16} c_{ij}^{(p)} dx^i dx^j = \frac{1}{16}\left[c_{ij}^{(1)} dx^i dx^j + c_{ij}^{(2)} dx^i dx^j + c_{ij}^{(3)} dx^i dx^j + c_{ij}^{(4)} dx^i dx^j + \right.$$

$$+ c_{ij}^{(5)} dx^i dx^j + c_{ij}^{(6)} dx^i dx^j + c_{ij}^{(7)} dx^i dx^j + c_{ij}^{(8)} dx^i dx^j +$$

$$+ c_{ij}^{(9)} dx^i dx^j + c_{ij}^{(10)} dx^i dx^j + c_{ij}^{(11)} dx^i dx^j + c_{ij}^{(12)} dx^i dx^j +$$

$$\left. + c_{ij}^{(13)} dx^i dx^j + c_{ij}^{(14)} dx^i dx^j + c_{ij}^{(15)} dx^i dx^j + c_{ij}^{(16)} dx^i dx^j \right] = 0, \tag{25}$$

then this expression can be used for an average flat $\lambda_{m,n}$-vacuum. At the same time, it is a condition for maintaining the $\lambda_{m,n}$-vacuum balance.

Recall that the "vacuum balance condition" was formulated in the introduction of the article [1], and this is the basic statement that, in particular, no matter what convex-concave curvatures (fluctuations) occur with the local area of the $\lambda_{m,n}$-vacuum, on average over the entire area they are equal to zero.

Preprints (www.preprints.org) | NOT PEER-REVIEWED | Posted: 5 October 2023 doi:10.20944/preprints202308.0570.v4

In this case, all 16×16=256 components of 16 averaged metric tensors $c_{ij}^{(p)}$ can be random functions of time. But, according to the condition of $\lambda_{m,n}$-vacuum balance, these metric-dynamic fluctuations should overflow into each other so that the total metric (25) on average remains equal to zero.

Based on the metric (25), $\lambda_{m,n}$-vacuum thermodynamics can be developed, which considers the most complex, near-zero "transfusions" of the local $\lambda_{m,n}$-vacuum curvatures. Concepts about $\lambda_{m,n}$-vacuum entropy and temperature (i.e., the essence of chaoticity and intensity of local $\lambda_{m,n}$-vacuum fluctuations) can be introduced. We can talk about the "cooling" of the $\lambda_{m,n}$-vacuum to "freezing", its "heating" to "evaporation" and many other effects similar to the processes occurring in atomistic continuous media.

Features of $\lambda_{m,n}$-vacuum thermodynamics are associated with processes when the gradients of $\lambda_{m,n}$-vacuum fluctuations approach the speed of light ($dc_{ij}^{(p)}/dx_a \sim c$) or zero ($dc_{ij}^{(p)}/dx_a \sim 0$). A detailed consideration of $\lambda_{m,n}$-vacuum thermodynamics and torsion fields is beyond the scope of this article. However, some aspects of this area of research are considered in [3–5].

2.4. The second stage of compactification of curved mathematical measurements

Just as it was done in §7.2 in [2], Ex. (25) can be reduced to two terms

$$\frac{1}{2}\left(\langle ds^{(+)2}\rangle + \langle ds^{(-)2}\rangle\right) = \frac{1}{2}\left(\langle g_{ij}^{(+)}\rangle dx^i dx^j + \langle g_{ij}^{(-)}\rangle dx^i dx^j\right) = 0, \tag{26}$$

where $$\left\langle g_{ij}^{(+)}\right\rangle dx^i dx^j = \left\langle g_{ij}^{(+---)}\right\rangle dx^i dx^j = \frac{1}{7}\sum_{p=1}^{7} c_{ij}^{(p)} dx^i dx^j, \text{ with signature } (+---) \tag{27}$$

is the quadratic form, which is the result of averaging seven metrics from the list (24) with signatures included in the numerator of the left rank (43) in [2] or (29);

$$\langle g_{ij}^{(-)}\rangle dx^i dx^j = \langle g_{ij}^{(-+++)}\rangle dx^i dx^j = \frac{1}{7}\sum_{q=8}^{14} c_{ij}^{(q)} dx^i dx^j, \text{ with signature } (-+++) \tag{28}$$

is the quadratic form, which is the result of averaging seven averaged metrics from the list (24) with signatures included in the numerator of the right rank (43) in [2] or (29).

$$\begin{array}{llll}
(+\ +\ +\ +) & + & (-\ -\ -\ -) & = 0 \\
(-\ -\ -\ +) & + & (+\ +\ +\ -) & = 0 \\
(+\ -\ -\ +) & + & (-\ +\ +\ -) & = 0 \\
(-\ -\ +\ -) & + & (+\ +\ -\ +) & = 0 \\
(+\ +\ -\ -) & + & (-\ -\ +\ +) & = 0 \\
(-\ +\ -\ -) & + & (+\ -\ +\ +) & = 0 \\
\underline{(+\ -\ +\ -)} & + & \underline{(-\ +\ -\ +)} & = 0 \\
(+\ -\ -\ -)_{+} & + & (-\ +\ +\ +)_{+} & = 0.
\end{array} \tag{29}$$

Thus, from the complex $\lambda_{m,n}$-vacuum fluctuations, two averaged sides can be distinguished:
1) the averaged "outer" side of the 2^3-$\lambda_{m,n}$-vacuum (or *subcont*, see §2.7 in [2]) with the averaged metric

$$\langle ds^{(\pm---)2}\rangle = \langle ds^{(+)2}\rangle = \langle g_{ij}^{(+)}\rangle dx^i dx^j, \text{ with signature } (+---), \tag{30}$$

where $$\langle g_{ij}^{(+)}\rangle dx^i dx^j = \langle g_{ij}^{(+---)}\rangle dx^i dx^j = \frac{1}{7}\sum_{p=1}^{7} c_{ij}^{(p)} dx^i dx^j, \tag{31}$$

here

$$g_{ij}^{(+)} = \begin{pmatrix} g_{00}^{(+)} & g_{10}^{(+)} & g_{20}^{(+)} & g_{30}^{(+)} \\ g_{01}^{(+)} & g_{11}^{(+)} & g_{21}^{(+)} & g_{31}^{(+)} \\ g_{02}^{(+)} & g_{12}^{(+)} & g_{22}^{(+)} & g_{31}^{(+)} \\ g_{03}^{(+)} & g_{13}^{(+)} & g_{23}^{(+)} & g_{33}^{(+)} \end{pmatrix} \tag{32}$$

are components of the metric tensor of the *subcont* (i.e., the "outer" side of the 2^3-$\lambda_{m,n}$-vacuum).

Preprints (www.preprints.org) | NOT PEER-REVIEWED | Posted: 5 October 2023 doi:10.20944/preprints202308.0570.v4

2) the averaged "inner" side of the 2^3-$\lambda_{m,n}$-vacuum (or *antisubcont*, see §2.7 in [2]) with the averaged metric

$$\langle ds^{(-+++)2}\rangle = \langle ds^{(-)2}\rangle = \langle g_{ij}^{(-)}\rangle dx^i dx^j, \text{ with signature } (-+++), \tag{33}$$

where

$$\langle g_{ij}^{(-)}\rangle dx^i dx^j = \langle g_{ij}^{(-+++)}\rangle dx^i dx^j = \frac{1}{7}\sum_{q=8}^{14} c_{ij}^{(q)} dx^i dx^j, \tag{34}$$

here

$$g_{ij}^{(-)} = \begin{pmatrix} g_{00}^{(-)} & g_{10}^{(-)} & g_{20}^{(-)} & g_{30}^{(-)} \\ g_{01}^{(-)} & g_{11}^{(-)} & g_{21}^{(-)} & g_{31}^{(-)} \\ g_{02}^{(-)} & g_{12}^{(-)} & g_{22}^{(-)} & g_{31}^{(-)} \\ g_{03}^{(-)} & g_{13}^{(-)} & g_{23}^{(-)} & g_{33}^{(-)} \end{pmatrix} \tag{35}$$

are the components of the metric tensor of the *antisubcont* (i.e., the "inner" side of the 2^3-$\lambda_{m,n}$-vacuum).

Recall that the two-sided model of $\lambda_{m,n}$-vacuum, that is, the result of averaging complex metric-dynamic fluctuations of $\lambda_{m,n}$-vacuum to a two-sided level of consideration, is called in §2.7 in [2] "2^3-$\lambda_{m,n}$-vacuum", because in this case, only $4+4=8=2^3$ mathematical measurements remain within the framework of consideration.

To shorten the notation, the averaging signs < > of the components of the metric tensors (32) and (35) are omitted.

Once again, we note that two concepts were formally introduced in [1]:

- *subcont* (i.e., the *substantial continuum* or the outer side of the 2^3-$\lambda_{m,n}$-vacuum with the averaged metric (30) and with the signature $(+---)$ of the Minkowski space);
- *antisubcont* (i.e., *antisubstantial continuum* or inner side of 2^3-$\lambda_{m,n}$-vacuum with averaged metric (33) and signature $(-+++)$ of Minkowski antispace).

The fictitious concepts of *subcont* and *antisubcont* are introduced to simplify and facilitate our perception of the complex intra-vacuum processes.

Thus, from the complexly fluctuating $\lambda_{m,n}$-vacuum (see Figure 6), due to simplification and averaging, we singled out only one averaged 2^3-$\lambda_{m,n}$-vacuum with two mutually opposite 4-dimensional sides: *subcont* and *antisubcont* (see Figure 7).

Figure 6. Fractal illustration of complex intra-vacuum processes.

Preprints (www.preprints.org) | NOT PEER-REVIEWED | Posted: 5 October 2023 doi:10.20944/preprints202308.0570.v4

On Figure 7 conditionally shows the average section of the two-sided 2^3-$\lambda_{m,n}$-vacuum, the outer side of which (*subcont*) is described by the averaged metric $\langle ds^{(+---)2}\rangle$(30), and the inner side (*antisubcont*) is described by the averaged metric $\langle ds^{(-+++)2}\rangle$ (33).

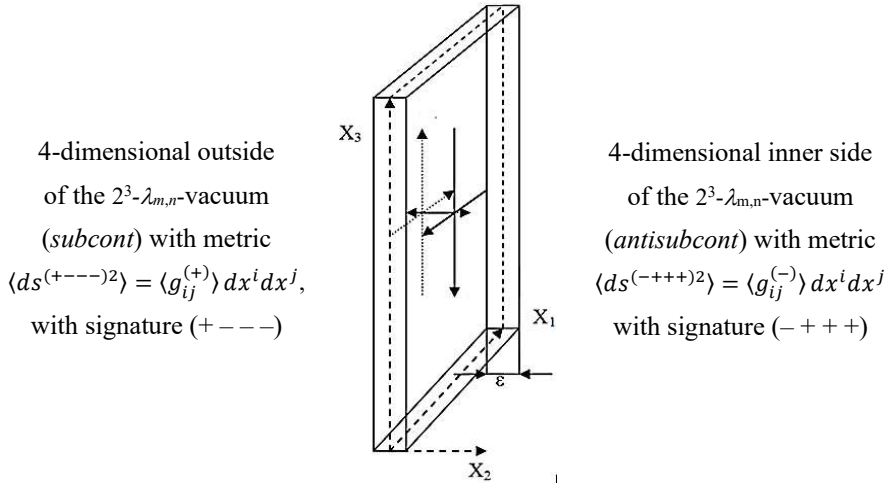

Figure 7. The simplified illustration of a two-sided section of the 2^3-$\lambda_{m\div n}$-vacuum, the outer side of which (*subcont*) is described by the averaged metric $\langle ds^{(+---)2}\rangle$ (30) with the signature (+ – – –), and its inner side (antisubcont) is described by the metric $\langle ds^{(-+++)2}\rangle$ (33) with the opposite signature (– + + +), as $\varepsilon \to 0$.

Let's explain the importance of at least two-sided consideration with a simple example. Let's take a sheet of paper and draw lines (segments) of the same length on its two sides in the same place (see Figure 8 *a,b*)

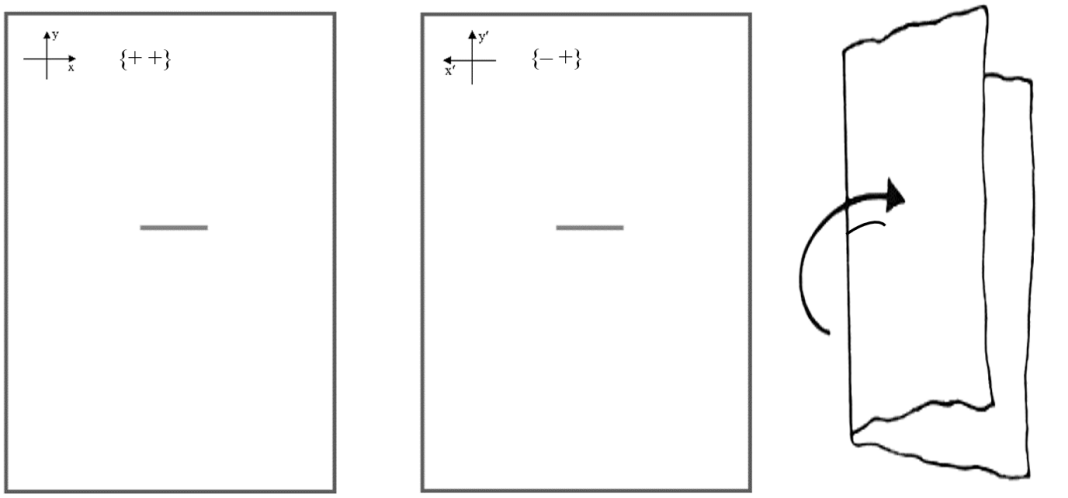

a)

The outer side of the sheet with stignature {+ +}

b)

The inner side of the sheet with stignature {– +}

c)

Curved sheet of paper

Figure 8. Two sides of one sheet of paper.

Reference systems XY or X'Y' on two opposite sides of a sheet of paper have different stignatures, respectively {+ +} and {+ –}. To understand this, take a sheet of paper and draw on it the XY reference system (as in Figure 8a). Then turn the sheet over, and on its reverse side depict the X'Y' reference system in the same way in the same place. If you compare these reference systems, you will find that the X and X' axes are directed in different directions, so their stignatures are different.

Preprints (www.preprints.org) | NOT PEER-REVIEWED | Posted: 5 October 2023 doi:10.20944/preprints202308.0570.v4

If the given sheet of paper is not curved, then the reference system with stignatures {+ +} and {+ –} are alike, i.e., any of them can set the coordinates of the drawn lines.

However, if this sheet is bent (see Figure 8*c*), then the line on the outer side of the sheet (see Figure 8a) will slightly expand, and the line on the inner side of the sheet (Figure 8*b*) will shrink by almost the same amount. In other words, the expansion of one line inevitably leads to the compression of another line drawn on the opposite side of the sheet.

Therefore, at least a two-sided consideration of the process of curvature of a sheet of paper is inevitable. Otherwise, one-sided consideration will lead not only to the loss of information about the process under study, but also in some cases to paradoxical and erroneous conclusions. In addition, the two-pronged approach immediately takes into account the vacuum balance condition, which states that any action is accompanied by a reaction. In the considered case, the expansion of one line is inevitably accompanied by compression of the other line, therefore, if we neglect the thickness of the sheet, then its average deformation of these lines tends to zero.

In fact, a sheet of paper has a thickness ε (see Figure 7). Therefore, in its thickness, one can always distinguish a cube with an edge length ε (see Figures 7 and 9).

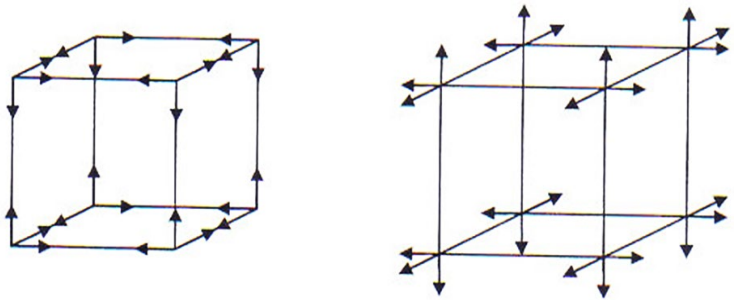

Figure 9. A cube isolated in the thickness of a sheet of paper (or in some other continuous medium, including vacuum).

If the sheet is bent, all sixteen 3-bases associated with the trihedral angles of such a deformed cube will be distorted in different ways (see Figure 4). Therefore, the Algebra of Signatures develops a mathematical apparatus that initially takes into account the distortions of all sixteen 3-bases at once, shown in Figure 9.

Only in the case when the thickness of a sheet of paper is so small that it can be neglected, it is permissible to simplify the problem to a two-sided consideration.

Unilateral consideration, i.e. the study of the curvature of only one side of a sheet of paper is possible, but will inevitably lead to a fundamental incompleteness of the mathematical model of the process under study.

In relation to vacuum physics, we are forced to state that the void (i.e., vacuum), which plays the role of the space surrounding us, has at least two sides: 1) external, i.e. Minkowski space with signature (+ – – –) and 2) internal, i.e. Minkowski antispace with signature (– + + +) (see Figure 7). One-sided consideration will inevitably lead to dead-ends and unfinished areas of scientific research.

For example, a metric that is a solution to the equations of the general theory of relativity (GR) of A. Einstein with the signature (+ – – –) can only describe a one-sided cosmological model of the Universe, which, in principle, cannot be completed. We also need, at a minimum, a metric-solution of the same equations with the opposite signature (– + + +). A more complete cosmological model should take into account all 16 metric-solutions of GR equations with signatures (29). Only such a cosmological model can claim logical completeness. The project of the cosmological model taking into account metric-solutions with all 16 possible signatures will be presented in subsequent articles of this project.

2.5. Four-strain tensor of 2^3-$\lambda_{m,n}$-vacuum in the case of a simplified two-sided consideration

2.5.1. Four-strain tensors of two sides of 2^3-$\lambda_{m,n}$-vacuum

Preprints (www.preprints.org) | NOT PEER-REVIEWED | Posted: 5 October 2023 doi:10.20944/preprints202308.0570.v4

Let's assume that the simplified two-sided model of the 2^3-$\lambda_{m,n}$-vacuum presented in the previous paragraph (see Figure 7) satisfies the given consideration accuracy.

Let the initial uncurved state of the studied area of the outer side of the 2^3-$\lambda_{m,n}$-vacuum (i.e., *subcont*) be characterized by a zero averaged metric (30)

$$ds_0^{(+---)2} = ds_0^{(+)2} = g_{ij0}^{(+)} dx^i dx^j, \text{ with signature } (+---). \tag{36}$$

Here and below, to shorten the entries, the averaging sign <> is removed, while it is conditionally assumed that

$$ds^{(+---)2} = \langle ds^{(+---)2} \rangle, \quad ds^{(+)2} = \langle ds^{(+)2} \rangle \text{ и } g_{ij}^{(+)} = \langle g_{ij}^{(+)} \rangle.$$

In the Cartesian coordinate system, metric (36) takes the form

$$ds_0^{(+)2} = c^2 dt^2 - dx^2 - dy^2 - dz^2, \tag{36a}$$

Wherein

$$g_{ij0}^{(+)} = \begin{pmatrix} 1 & 0 & 0 & 0 \\ 0 & -1 & 0 & 0 \\ 0 & 0 & -1 & 0 \\ 0 & 0 & 0 & -1 \end{pmatrix}. \tag{37}$$

In the case of curvature of the same section of the *subcont*, its metric-dynamic state is determined by the averaged metric

$$ds^{(+---)2} = ds^{(+)2} = g_{ij}^{(+)} dx^i dx^j, \text{ with signature } (+---). \tag{38}$$

The difference between the curved state of the studied section of the *subcont* and its non-curved state is determined by the Expression [3]

$$ds^{(+)2} - ds_0^{(+)2} = \left(g_{ij}^{(+)} - g_{ij0}^{(+)}\right) dx^i dx^j = 2\varepsilon_{ij}^{(+)} dx^i dx^j, \tag{39}$$

here

$$\varepsilon_{ij}^{(+)} = \tfrac{1}{2}\left(g_{ij}^{(+)} - g_{ij0}^{(+)}\right) \tag{40}$$

is the 4-deformation tensor of the local section of the *subcont*.

The relative elongation (or contraction) of the curved section of the *subcont* is [3]

$$l^{(+)} = \frac{ds^{(+)} - ds_0^{(+)}}{ds_0^{(+)}} = \frac{ds^{(+)}}{ds_0^{(+)}} - 1. \tag{41}$$

Whence it follows

$$ds^{(+)2} = (1 + l^{(+)})^2 ds_0^{(+)2}. \tag{42}$$

Substituting (42) into (39), taking into account (40), we obtain [3]

$$\varepsilon_{ij}{}^{(+)} = \tfrac{1}{2}\left[(1 + l^{(+)})^2 - 1\right] g_{ij0}^{(+)}, \tag{43}$$

or expanded

$$\varepsilon_{ij}{}^{(+)} = \tfrac{1}{2}\left[(1 + l_i{}^{(+)})(1 + l_j{}^{(+)}) \cos\beta_{ij}{}^{(+)} - \cos\beta_{ij0}{}^{(+)}\right] g_{ij0}^{(+)}, \tag{44}$$

where

$\beta_{ij0}{}^{(+)}$ is the angle between the axes x^i and x^j of the reference system, "frozen" into the initial uncurved state of the *subcont* section under study;

$\beta_{ij}{}^{(+)}$ is the angle between the axes $x^{i\prime}$and $x^{j\prime}$ of the distorted reference system "frozen" into the distorted state of the same section of the *subcont*.

When $\beta_{ij0}{}^{(+)} = \pi/2$, Ex. (44) takes the form

Preprints (www.preprints.org) | NOT PEER-REVIEWED | Posted: 5 October 2023 doi:10.20944/preprints202308.0570.v4

$$\varepsilon_{ij}^{(+)} = ½\,[(1 + l_i^{(+)})(1 + l_j^{(+)})\cos\beta_{ij}^{(+)} - 1]\;\; g_{ij0}^{(+)}. \tag{45}$$

For the diagonal components of the 4-strain tensor $\varepsilon_{ii}^{(+)}$, Ex. (45) is simplified

$$\varepsilon_{ii}^{(+)} = ½\,[(1 + l_i^{(+)})^2 - 1]\;\; g_{ij0}^{(+)}, \tag{46}$$

whence follows [3]

$$l_i^{(+)} = \sqrt{1 + \frac{2\varepsilon_{ii}^{(+)}}{g_{ii0}^{(+)}}} - 1 = \sqrt{1 + \frac{g_{ii}^{(+)} - g_{ii0}^{(+)}}{g_{ii0}^{(+)}}} - 1 = \sqrt{\frac{g_{ii}^{(+)}}{g_{ii0}^{(+)}}} - 1. \tag{47}$$

If deformations of the *subcont* section $\varepsilon_{ij}^{(+)}$ are small, then, expanding Ex. (47) into a series, and, confining ourselves to the first member of this series, we obtain the relative elongation of the local *subcont* section [3]

$$l_i^{(+)} \approx \frac{\varepsilon_{ii}^{(+)}}{g_{ii0}^{(+)}}. \tag{48}$$

Similarly, the deformation of the local section of the inner side of the 2^3-$\lambda_{m,n}$-vacuum (*antisubcont*) is determined by the Expression

$$ds^{(-)2} - ds_0^{(-)2} = \left(g_{ij}^{(-)} - g_{ij0}^{(-)}\right)dx^i dx^j = 2\varepsilon_{ij}^{(-)}dx^i dx^j, \tag{49}$$

Where

$$\varepsilon_{ij}^{(-)} = ½\left(g_{ij}^{(-)} - g_{ij0}^{(-)}\right) \tag{50}$$

is the 4-deformation tensor of the local section of the *antisubcont*;

$$ds_0^{(-+++)2} = ds_0^{(-)2} = g_{ij0}^{(-)}dx^i dx^j, \text{ with signature } (-+++) \tag{51}$$

is the metric of the uncurved state of the local section of the *antisubcont*. In the Cartesian coordinate system, metric (51) takes the form

$$s_0^{(-)2} = -c^2dt^2 + dx^2 + dy^2 + dz^2, \tag{51a}$$

where

$$g_{ij0}^{(-)} = \begin{pmatrix} -1 & 0 & 0 & 0 \\ 0 & 1 & 0 & 0 \\ 0 & 0 & 1 & 0 \\ 0 & 0 & 0 & 1 \end{pmatrix}; \tag{51b}$$

in its turn $ds^{(-+++)2} = ds^{(-)2} = g_{ij}^{(-)}dx^i dx^j$, with the same signature $(-+++)$ (52)

is the metric of the curved local section of the *antisubcont*.

The relative elongation (or contraction) of the local section of the *antisubcont* is determined by the Expression

$$l^{(-)} = \frac{ds^{(-)} - ds_0^{(-)}}{ds_0^{(-)}} = \frac{ds^{(-)}}{ds_0^{(-)}} - 1. \tag{53}$$

2.5.2. *The 4-strain tensor of 2^3-$\lambda_{m,n}$-vacuum in the case of two-sided consideration*

We define the 4-strain tensor of a local section of a two-sided 2^3-$\lambda_{m,n}$-vacuum as the average value of the deformations of its two sides

$$\varepsilon_{ij}^{(\pm)} = ½\,(\varepsilon_{ij}^{(+)} + \varepsilon_{ij}^{(-)}) = ½\,(\varepsilon_{ij}^{(+---)} + \varepsilon_{ij}^{(-+++)}), \tag{54}$$

or, taking into account expressions (40) and (50), we obtain

$$\varepsilon_{ij}^{(\pm)} = ½\,(g_{ij}^{(+)} + g_{ij}^{(-)}) - ½\,(g_{ij0}^{(+)} + g_{ij0}^{(-)}) = ½\,(g_{ij}^{(+)} + g_{ij}^{(-)}), \tag{55}$$

Preprints (www.preprints.org) | NOT PEER-REVIEWED | Posted: 5 October 2023 doi:10.20944/preprints202308.0570.v4

because from the condition of 2^3-$\lambda_{m,n}$-vacuum balance (48) in [2] $ds^{(+---)2} + ds^{(-+++)2} = 0$ follows:

$$g_{ij0}^{(+)} + g_{ij0}^{(-)} = g_{ij0}^{(+---)} + g_{ij0}^{(-+++)} = 0. \tag{56}$$

The relative elongation (or contraction) $l_i^{(\pm)}$ of the local section of the two-sided 2^3-$\lambda_{m,n}$-vacuum is determined by the Expression

$$l_i^{(\pm)} = {}^1\!/_2 \left(l_i^{(+)} + l_i^{(-)}\right) \tag{57}$$

where

$$l_i^{(+)} = \sqrt{1 + \frac{2\varepsilon_{ii}^{(\pm)}}{g_{ii0}^{(+)}}} - 1 = \sqrt{1 + \frac{g_{ii}^{(+)} + g_{ii}^{(-)}}{g_{ii0}^{(+)}}} - 1, \tag{58}$$

$$l_i^{(-)} = \sqrt{1 + \frac{2\varepsilon_{ii}^{(\pm)}}{g_{ii0}^{(-)}}} - 1 = \sqrt{1 + \frac{g_{ii}^{(+)} + g_{ii}^{(-)}}{g_{ii0}^{(-)}}} - 1 = \sqrt{1 - \frac{g_{ii}^{(+)} + g_{ii}^{(-)}}{g_{ii0}^{(+)}}} - 1, \tag{59}$$

because according to the condition of the $\lambda_{m,n}$-vacuum balance (56) $g_{ij0}^{(-)} = -g_{ij0}^{(+)}$.

Substituting Exs. (58) and (59) into Ex. (57), we obtain

$$l_i^{(\pm)} = {}^1\!/_2 \left(\sqrt{1 + \frac{g_{ii}^{(+)} + g_{ii}^{(-)}}{g_{ii0}^{(+)}}} + \sqrt{1 - \frac{g_{ii}^{(+)} + g_{ii}^{(-)}}{g_{ii0}^{(+)}}} \right) - 1. \tag{60}$$

It can be seen from this Expression that the relative elongation (or contraction) of the local section of the two-sided 2^3-$\lambda_{m,n}$-vacuum, $l_i^{(\pm)}$ can be a complex number.

In this regard, we note the following important circumstance. If both sides of Ex. (55) are multiplied by $dx^i dx^j$, then we obtain the averaged quadratic form

$$ds^{(\pm)2} = {}^1\!/_2 \left(ds^{(+)2} + ds^{(-)2}\right) = {}^1\!/_2 \left(ds^{(+---)2} + ds^{(-+++)2}\right), \tag{61}$$

which resembles the Pythagorean theorem $c^2 = a^2 + b^2$.

This means that the line segments $({}^1\!/_2)^{1/2} ds^{(+)}$ and $({}^1\!/_2)^{1/2} ds^{(-)}$, which lie on two mutually opposite sides of the two-sided 2^3-$\lambda_{m,n}$-vacuum, are always mutually perpendicular to each other, i.e. $ds^{(+)} \perp ds^{(-)}$ (Figure 10*a*).

In this case, two lines directed in the same direction can always be mutually perpendicular only if they form a double helix (see Figures 10*b* and 12).

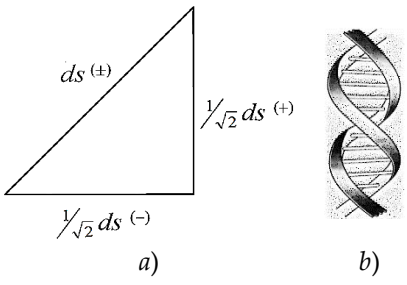

Figure 10. a) Mutually perpendicular segments $({}^1\!/_2)^{1/2} ds^{(+)}$ and $({}^1\!/_2)^{1/2} ds^{(-)}$; *b*) If you project a double helix onto a plane, then at the intersection of its lines $ds^{(+)}$ and $ds^{(-)}$ are always mutually perpendicular.

Thus, the averaged metric (61) corresponds to a "braid" segment consisting of two mutually perpendicular spirals $s^{(+)}$ and $s^{(-)}$. In this case, just like the relative elongation of the local section of the two-sided 2^3-$\lambda_{m,n}$-vacuum $l_i^{(\pm)}$ (60), such a section of the "double helix" can be described by a complex number

$$ds^{(\pm)} = {}^1\!/_{\sqrt{2}} \left(ds^{(+)} + i ds^{(-)}\right),$$

Preprints (www.preprints.org) | NOT PEER-REVIEWED | Posted: 5 October 2023 doi:10.20944/preprints202308.0570.v4

the square of whose modulus is equal to Ex. (61).

Below, a k-braid is the result of averaging metrics with different signatures (where k is the number of averaged metrics, i.e., the number of "threads" in the "braid"). For example, the averaged metric (61) is called a 2-braid, since it is "twisted" from 2 lines : $ds^{(+)} = ds^{(+---)}$ and $ds^{(-)} = ds^{(-+++)}$.

Here is another augment in favor of the mutual perpendicularity of the segments $ds^{(+)}$ and $ds^{(-)}$;

Figure 8 showed that the reference systems XY or X'Y' on two opposite sides of a sheet of paper have different stignatures {+ +} and {+ –}. In order to get a completely opposite stignature {– –}, it is necessary first to depict the reference system XY on the sheet, then turn this sheet 90 degrees clockwise, then turn it to the other side and similarly draw the reference system X'Y' on the same place where the reference system XY (see Figure 11). The result will be a reference system Y'X' with a completely opposite stignature {– –} in relation to the XY system.

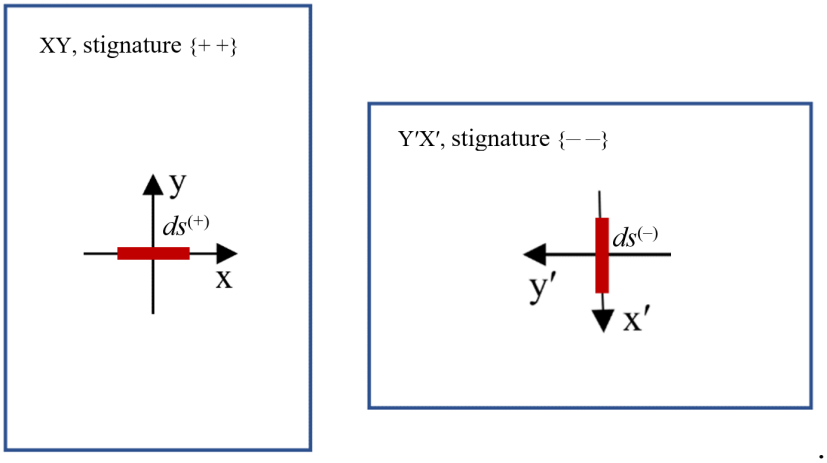

Figure 11. Two sides of the space with completely opposite stignatures {+ +} and {– –}.

If, on one side of the sheet, draw a line $ds^{(+)}$ along the X axis (see Figure 11), and on the other completely opposite side, draw the same line $ds^{(-)}$ along the X' axis, then it turns out that the lines $ds^{(+)}$ and $ds^{(-)}$ are mutually perpendicular. Such a crossing of the $ds^{(+)}$ and $ds^{(-)}$ lines takes place in each local area of the sheet, which resembles the crossing of fabric threads (see Figure 12*a*).

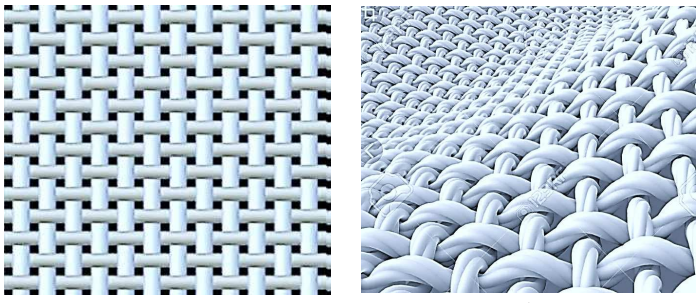

(*a*) (*b*)

Figure 12. Woven threads of the fabric.

If a hypothetical sheet with two completely opposite sides (i.e., with opposite stignatures {+ +} and {– –}) is bent as shown in Figure 8*c*, then the line $ds^{(+)}$ will stretch, and the corresponding line $ds^{(-)}$ on the other side of such a sheet will remain the same (i.e., not deformed). In this case, the line will shrink on the perpendicular axis Y'. This ultimately leads to the twisting of the $ds^{(+)}$ and $ds^{(-)}$ lines into spiral bundles (see Figures 10 and 12a).

As applied to the model of the two-sided section of the 2^3-$\lambda_{m,n}$-vacuum with completely opposite sides, i.e. with signatures (+ – – –) and (– + + +) (Figure 7), we conclude that the intertwined lines $ds^{(+---)}$ and $ds^{(-+++)}$ form a fabric of 3-dimensional extent. In other words, the 2^3-$\lambda_{m,n}$-vacuum is not just

Preprints (www.preprints.org) | NOT PEER-REVIEWED | Posted: 5 October 2023 doi:10.20944/preprints202308.0570.v4

a two-sided 8-dimensional space, but is the result of the interlacing of its two sides, like the threads of a fabric (see Figure 12*b*).

Deformation of one side of such length inevitably leads to a perpendicular counter - response on its other side. This is the reason for the folding of local sections of such a two-sided space into double helixes (see Figure 10 *a,b* and Figure 12*b*).

It is difficult to imagine a 3-dimensional tissue structure of a two-sided 8-dimensional 2^3-$\lambda_{m\div n}$-vacuum, but the mathematics of the Algebra of Signatures takes into account the ubiquitous interweaving of the lines $ds^{(+---)}$ and $ds^{(-+++)}$ automatically, since not summed these lines themselves, but their quadratic forms $ds^{(+---)2}$ and $ds^{(-+++)2}$ (61), which define the metrics of these extensions.

2.5.3. *The 4-strain tensor of a curved 2^6-$\lambda_{m,n}$-vacuum in the case of sixteen-sided consideration*

At the next deeper 16-sided level of consideration, the number of mathematical dimensions is 16 × 4 = 64 = 2^6, so at this level the subject of consideration is the 2^6-$\lambda_{m,n}$-vacuum.

The metric-dynamic properties of the local region of the 2^6-$\lambda_{m,n}$-vacuum are characterized by a superposition (i.e., additive superposition or averaging) of sixteen metrics with all 16 possible signatures (29), i.e. 16-braid (according to the definition of *k*-braid after Ex. (61)):

$$\begin{aligned} ds_\Sigma{}^2 = 1/16\ (&ds^{(+---)2} + ds^{(++++)2} + ds^{(---+)2} + ds^{(+--+)2} + \\ &+ ds^{(--+-)2} + ds^{(+++-)2} + ds^{(++--)2} + ds^{(-+--)2} + ds^{(+-+-)2} + \\ &+ ds^{(-+++)2} + ds^{(----)2} + ds^{(+++-)2} + ds^{(-++-)2} + \\ &+ ds^{(++-+)2} + ds^{(--++)2} + ds^{(+-++)2} + ds^{(-+-+)2}). \end{aligned} \tag{62}$$

In this case, we have 16 4-deformation tensors of all 16 types of curved 4-spaces with different signatures (or topologies, see §2.4 in [2])

$$\varepsilon_{ij}^{(p)} = \begin{pmatrix} \varepsilon_{ij}^{(1)} & \varepsilon_{ij}^{(2)} & \varepsilon_{ij}^{(3)} & \varepsilon_{ij}^{(4)} \\ \varepsilon_{ij}^{(5)} & \varepsilon_{ij}^{(6)} & \varepsilon_{ij}^{(7)} & \varepsilon_{ij}^{(8)} \\ \varepsilon_{ij}^{(9)} & \varepsilon_{ij}^{(10)} & \varepsilon_{ij}^{(11)} & \varepsilon_{ij}^{(12)} \\ \varepsilon_{ij}^{(13)} & \varepsilon_{ij}^{(14)} & \varepsilon_{ij}^{(15)} & \varepsilon_{ij}^{(16)} \end{pmatrix}, \tag{63}$$

where according to expression (25)

$$\varepsilon_{ij}{}^{(p)} = \ \tfrac{1}{2}\ (c_{ij}{}^{(p)} - c_{ij0}{}^{(p)}) \tag{64}$$

is the 4-deformation tensor of the *p*-th 4-space, $p = 1,2,\ldots,16$, where:

$c_{ij0}{}^{(p)}$ is the metric tensor of the non-curved region of the *p*-th 4-space with the corresponding signature;
$c_{ij}{}^{(p)}$ is the metric tensor of the same but curved region of the *p*-th 4-space with the same signature.

By analogy with Ex. (54), at the 16-sided level of consideration, the general tensor of 4-deformations $\varepsilon_{ij\,\Sigma}^{(16)}$ of the local curved region of the 2^6-$\lambda_{m,n}$-vacuum is defined as the average value

$$\varepsilon_{ij\,\Sigma}^{(16)} = \frac{1}{16}\left(\varepsilon_{ij}^{(1)} + \varepsilon_{ij}^{(2)} + \varepsilon_{ij}^{(3)} + \cdots + \varepsilon_{ij}^{(16)}\right) = \frac{1}{16}\sum_{p=1}^{16} \varepsilon_{ij}^{(p)}. \tag{65}$$

In this case, the relative elongation of the local region of the 2^6-$\lambda_{m,n}$-vacuum $l_{i\,\Sigma}^{(16)}$ in this case is given by the average hypercomplex number of the 16-th rank

$$l_{i\,\Sigma}^{(16)} = 1/\sqrt{16}\ \ (\eta_1 l_i{}^{(1)} + \eta_2 l_i{}^{(2)} + \eta_3 l_i{}^{(3)} + \ldots + \eta_{16} l_i{}^{(16)}), \tag{66}$$

where

$$l_i^{(p)} = \sqrt{1 + \frac{2\varepsilon_{ii}^{(p)}}{c_{ii}^{0(p)}}} - 1, \tag{67}$$

Preprints (www.preprints.org) | NOT PEER-REVIEWED | Posted: 5 October 2023 doi:10.20944/preprints202308.0570.v4

η_m is an orthonormal basis of 16 unit objects (m = 1,2,3,…,16) satisfying the anticommutation relation of the Clifford algebra

$$\eta_m\eta_n + \eta_n\eta_m = 2\delta_{mn}\,, \tag{68}$$

where δ_{nm} is the identity 16×16-matrix.

In this case, the curved section of the 16-braid consists of sixteen intertwined "colored" lines (threads):

$$\begin{aligned} ds_{(16)} = 1/\sqrt{16}\ (&\eta_1 ds^{(+---)} + \eta_2 ds^{(++++)} + \eta_3 ds^{(---+)} + \eta_4 ds^{(+--+)} + \\ &+ \eta_5 ds^{(--+-)} + \eta_6 ds^{(++--)} + \eta_7 ds^{(-+--)} + \eta_8 ds^{(+--+)} + \\ &+ \eta_9 ds^{(-+++)} + \eta_{10} ds^{(----)} + \eta_{11} ds^{(+++-)} + \eta_{12} ds^{(-++-)} + \\ &+ \eta_{13} ds^{(++-+)} + \eta_{14} ds^{(--++)} + \eta_{15} ds^{(+-++)} + \eta_{16} ds^{(-+--+)}). \end{aligned} \tag{69}$$

The colors of these lines conditionally correspond to the colors of the signatures (i.e., the types of topologies of these 4-dimensional spaces), which are formally assigned to these spaces in the framework of vacuum chromodynamics:

Red	(+ + + +) + (– – – –)	Anti-red
Yellow	(– – – +) + (+ + + –)	Anti-yellow
Orange	(+ – – +) + (– + + –)	Anti-orange
Green	(– – + –) + (+ + – +)	Anti-green
Blue	(+ + – –) + (– – + +)	Anti-blue
Dark blue	(– + – –) + (+ – + +)	Anti-dark blue
Violet	(+ – + –) + (– + – +)	Anti-violet
White	(+ – – –)$_+$ + (– + + +)$_+$	Black

(70)

Formal coloring of 16 lines (or threads) $ds^{(+---)}$, $ds^{(-+++)}$, $ds^{(++++)}$, $ds^{(++-+)}$, … , $ds^{(-+-+)}$ makes it possible to represent the "fabric" of 2^6-$\lambda_{m,n}$-vacuum woven from them in color form (Figures 6 &13).

Figure 13. Fractal illustration of a warped 2^6-$\lambda_{m,n}$-vacuum fabric woven from 16 "color" lines (threads).

Each "colored" 4-space with the corresponding signature (i.e., topology) (70) can be formally represented as a continuous plastic-elastic medium of the corresponding color. Such 4-spaces, which have elastoplastic properties, can be interpreted as "colored" ethers. But unlike the ether theory, in the geometrized vacuum physics based on the Algebra of Signatures (Alsigna), there is not one ether, but depending on the level of consideration, there can be 2 such ethers ("white" and "black") or 2^4 = 16 (with "colors" (70)) or 2^8 = 256 (with different shades of colors (70)) etc. to infinity. At the same

Preprints (www.preprints.org) | NOT PEER-REVIEWED | Posted: 5 October 2023 doi:10.20944/preprints202308.0570.v4

time, all these formal "colored" ethers of Alsigna are intertwined into a single 3-dimensional "carpet" (see Figures 6 and 14), i.e. form a single intertwined and seething 3-dimensional space. Such a 3-dimensional, mean-flat (i.e., "zero") space in each local area resembles a multi-dimensional Calabi-Yau manifold. In addition, the "colored" ethers of Alsigna are illusory in nature and are intended only to facilitate the perception and awareness of the most complex intra-vacuum processes.

If all curved linear forms $ds^{(+---)}$, $ds^{(-+++)}$, $ds^{(++-+)}$, … , $ds^{(-+-+)}$ can be represented in a diagonal form, then in accordance with (65) and (66) in [2], Ex. (69) can be represented in the spintensor form

(71)

$$
\begin{aligned}
ds^{(16)} = \frac{1}{\sqrt{16}}\Bigg[& \sqrt{g_{00}^{(1)}}dx_0\begin{pmatrix}1 & 0\\ 0 & -1\end{pmatrix} + \sqrt{g_{11}^{(1)}}dx_1\begin{pmatrix}0 & -i\\ i & 0\end{pmatrix} + \sqrt{g_{22}^{(1)}}dx_2\begin{pmatrix}0 & -1\\ 1 & 0\end{pmatrix} + \sqrt{g_{33}^{(1)}}dx_3\begin{pmatrix}i & 0\\ 0 & -i\end{pmatrix} + \\
& + \sqrt{g_{00}^{(2)}}dx_0\begin{pmatrix}-1 & 0\\ 0 & 1\end{pmatrix} + \sqrt{g_{11}^{(2)}}dx_1\begin{pmatrix}0 & -1\\ 1 & 0\end{pmatrix} + \sqrt{g_{22}^{(2)}}dx_2\begin{pmatrix}0 & -i\\ i & 0\end{pmatrix} + \sqrt{g_{33}^{(2)}}dx_3\begin{pmatrix}-i & 0\\ 0 & i\end{pmatrix} + \\
& + \sqrt{g_{00}^{(3)}}dx_0\begin{pmatrix}1 & 0\\ 0 & -1\end{pmatrix} + \sqrt{g_{11}^{(3)}}dx_1\begin{pmatrix}0 & i\\ -i & 0\end{pmatrix} + \sqrt{g_{22}^{(3)}}dx_2\begin{pmatrix}0 & 1\\ -1 & 0\end{pmatrix} + \sqrt{g_{33}^{(3)}}dx_3\begin{pmatrix}1 & 0\\ 0 & -1\end{pmatrix} + \\
& + \sqrt{g_{00}^{(4)}}dx_0\begin{pmatrix}-1 & 0\\ 0 & 1\end{pmatrix} + \sqrt{g_{11}^{(4)}}x_1\begin{pmatrix}0 & 1\\ -1 & 0\end{pmatrix} + \sqrt{g_{22}^{(4)}}x_2\begin{pmatrix}0 & -1\\ 1 & 0\end{pmatrix} + \sqrt{g_{33}^{(4)}}x_3\begin{pmatrix}-1 & 0\\ 0 & 1\end{pmatrix} + \\
& + \sqrt{g_{00}^{(5)}}dx_0\begin{pmatrix}1 & 0\\ 0 & -1\end{pmatrix} + \sqrt{g_{11}^{(5)}}dx_1\begin{pmatrix}0 & -i\\ i & 0\end{pmatrix} + \sqrt{g_{22}^{(5)}}dx_2\begin{pmatrix}0 & 1\\ -1 & 0\end{pmatrix} + \sqrt{g_{33}^{(5)}}dx_3\begin{pmatrix}i & 0\\ 0 & i\end{pmatrix} + \\
& + \sqrt{g_{00}^{(6)}}dx_0\begin{pmatrix}-1 & 0\\ 0 & 1\end{pmatrix} + \sqrt{g_{11}^{(6)}}dx_1\begin{pmatrix}0 & -1\\ 1 & 0\end{pmatrix} + \sqrt{g_{22}^{(6)}}dx_2\begin{pmatrix}0 & i\\ -i & 0\end{pmatrix} + \sqrt{g_{33}^{(6)}}dx_3\begin{pmatrix}-1 & 0\\ 0 & 1\end{pmatrix} + \\
& + \sqrt{g_{00}^{(7)}}dx_0\begin{pmatrix}1 & 0\\ 0 & -1\end{pmatrix} + \sqrt{g_{11}^{(7)}}dx_1\begin{pmatrix}0 & 1\\ -1 & 0\end{pmatrix} + \sqrt{g_{22}^{(7)}}dx_2\begin{pmatrix}0 & -1\\ 1 & 0\end{pmatrix} + \sqrt{g_{33}^{(7)}}dx_3\begin{pmatrix}-i & 0\\ 0 & -i\end{pmatrix} + \\
& + \sqrt{g_{00}^{(8)}}dx_0\begin{pmatrix}-1 & 0\\ 0 & 1\end{pmatrix} + \sqrt{g_{11}^{(8)}}dx_1\begin{pmatrix}0 & -1\\ 1 & 0\end{pmatrix} + \sqrt{g_{22}^{(8)}}dx_2\begin{pmatrix}0 & 1\\ -1 & 0\end{pmatrix} + \sqrt{g_{33}^{(8)}}dx_3\begin{pmatrix}i & 0\\ 0 & -i\end{pmatrix} + \\
& + \sqrt{g_{00}^{(9)}}dx_0\begin{pmatrix}1 & 0\\ 0 & -1\end{pmatrix} + \sqrt{g_{11}^{(9)}}dx_1\begin{pmatrix}0 & i\\ -i & 0\end{pmatrix} + \sqrt{g_{22}^{(9)}}dx_2\begin{pmatrix}0 & -1\\ 1 & 0\end{pmatrix} + \sqrt{g_{33}^{(9)}}dx_3\begin{pmatrix}1 & 0\\ 0 & -1\end{pmatrix} + \\
& + \sqrt{g_{00}^{(10)}}dx_0\begin{pmatrix}-1 & 0\\ 0 & 1\end{pmatrix} + \sqrt{g_{11}^{(10)}}dx_1\begin{pmatrix}0 & 1\\ -1 & 0\end{pmatrix} + \sqrt{g_{22}^{(10)}}dx_2\begin{pmatrix}0 & 1\\ -1 & 0\end{pmatrix} + \sqrt{g_{33}^{(10)}}dx_3\begin{pmatrix}-i & 0\\ 0 & i\end{pmatrix} + \\
& + \sqrt{g_{00}^{(11)}}dx_0\begin{pmatrix}1 & 0\\ 0 & -1\end{pmatrix} + \sqrt{g_{11}^{(11)}}dx_1\begin{pmatrix}0 & -i\\ i & 0\end{pmatrix} + \sqrt{g_{22}^{(11)}}dx_2\begin{pmatrix}0 & -1\\ 1 & 0\end{pmatrix} + \sqrt{g_{33}^{(11)}}dx_3\begin{pmatrix}1 & 0\\ 0 & 1\end{pmatrix} + \\
& + \sqrt{g_{00}^{(12)}}dx_0\begin{pmatrix}-1 & 0\\ 0 & 1\end{pmatrix} + \sqrt{g_{11}^{(12)}}dx_1\begin{pmatrix}0 & -1\\ 1 & 0\end{pmatrix} + \sqrt{g_{22}^{(12)}}dx_2\begin{pmatrix}0 & 1\\ -1 & 0\end{pmatrix} + \sqrt{g_{33}^{(12)}}dx_3\begin{pmatrix}-1 & 0\\ 0 & -1\end{pmatrix} + \\
& + \sqrt{g_{00}^{(13)}}dx_0\begin{pmatrix}1 & 0\\ 0 & -1\end{pmatrix} + \sqrt{g_{11}^{(13)}}dx_1\begin{pmatrix}0 & i\\ -i & 0\end{pmatrix} + \sqrt{g_{22}^{(13)}}dx_2\begin{pmatrix}0 & -i\\ -i & 0\end{pmatrix} + \sqrt{g_{33}^{(13)}}dx_3\begin{pmatrix}-1 & 0\\ 0 & 1\end{pmatrix} + \\
& + \sqrt{g_{00}^{(14)}}dx_0\begin{pmatrix}-1 & 0\\ 0 & 1\end{pmatrix} + \sqrt{g_{11}^{(14)}}dx_1\begin{pmatrix}0 & 1\\ -1 & 0\end{pmatrix} + \sqrt{g_{22}^{(14)}}dx_2\begin{pmatrix}0 & -1\\ 1 & 0\end{pmatrix} + \sqrt{g_{33}^{(14)}}dx_3\begin{pmatrix}-i & 0\\ 0 & -i\end{pmatrix} + \\
& + \sqrt{g_{00}^{(15)}}dx_0\begin{pmatrix}1 & 0\\ 0 & -1\end{pmatrix} + \sqrt{g_{00}^{(15)}}dx_1\begin{pmatrix}0 & -1\\ 1 & 0\end{pmatrix} + \sqrt{g_{00}^{(15)}}dx_2\begin{pmatrix}0 & 1\\ -1 & 0\end{pmatrix} + \sqrt{g_{00}^{(15)}}dx_3\begin{pmatrix}1 & 0\\ 0 & -1\end{pmatrix} + \\
& + \sqrt{g_{00}^{(16)}}dx_0\begin{pmatrix}-1 & 0\\ 0 & 1\end{pmatrix} + \sqrt{g_{11}^{(16)}}dx_1\begin{pmatrix}0 & 1\\ -1 & 0\end{pmatrix} + \sqrt{g_{22}^{(16)}}dx_2\begin{pmatrix}0 & i\\ i & 0\end{pmatrix} + \sqrt{g_{33}^{(16)}}dx_3\begin{pmatrix}i & 0\\ 0 & i\end{pmatrix}\Bigg]
\end{aligned}
$$

Within the framework of the Algebra of Signatures, much deeper 2^n-sided levels of consideration of the metric-dynamic properties of the curved region of the $\lambda_{m,n}$-vacuum are possible, while the number of components of the metric tensor characterizing its metric-dynamic properties can increase to infinity (see §2.9 in [2]).

6. Physical meaning of the components of the metric tensor

Preprints (www.preprints.org) | NOT PEER-REVIEWED | Posted: 5 October 2023 doi:10.20944/preprints202308.0570.v4

6.1. Nonzero components of the metric tensor

Let the averaged metric-dynamic states of two 4-dimensional sides of the local region of the 2^3-$\lambda_{m,n}$-vacuum be given by metrics (30) and (33) (see Figure 7). Consider the nonzero components of the metric tensors (32) and (35) of these metrics

$$g_{\alpha\beta}^{(+)} = \begin{pmatrix} \cdots & \cdots & \cdots & \cdots \\ \cdots & g_{11}^{(+)} & g_{21}^{(+)} & g_{31}^{(+)} \\ \cdots & g_{12}^{(+)} & g_{22}^{(+)} & g_{31}^{(+)} \\ \cdots & g_{13}^{(+)} & g_{23}^{(+)} & g_{33}^{(+)} \end{pmatrix}, \qquad g_{\alpha\beta}^{(-)} = \begin{pmatrix} \cdots & \cdots & \cdots & \cdots \\ \cdots & g_{11}^{(-)} & g_{21}^{(-)} & g_{31}^{(-)} \\ \cdots & g_{12}^{(-)} & g_{22}^{(-)} & g_{31}^{(-)} \\ \cdots & g_{13}^{(-)} & g_{23}^{(-)} & g_{33}^{(-)} \end{pmatrix}, \tag{72}$$

here the Greek alphabet indices α, β correspond to the 3-dimensional consideration (i.e., α, β = 1,2,3).

The scalar curvature of the local two-sided region of the 2^3-$\lambda_{m,n}$-vacuum in the framework of the Algebra of Signatures is determined by the complex number [6]

$$R^{(\pm)} = R^{(+)} + iR^{(-)}, \tag{73}$$

$$\left|R^{(\pm)}\right| = \sqrt{R^{(+)2} + R^{(-)2}}, \tag{74}$$

$$\varphi = arctg\left(\frac{R^{(-)}}{R^{(+)}}\right), \tag{75}$$

where the scalar curvature of each of the two sides of the 2^3-$\lambda_{m,n}$-vacuum is defined in the same way as in general relativity (GR)

$$R^{(+)} = g^{\alpha\beta(+)}R_{\alpha\beta}^{(+)} \quad \text{и} \quad R^{(-)} = g^{\alpha\beta(-)}R_{\alpha\beta}^{(-)}, \tag{76}$$

where

$$R_{\alpha\beta}^{(+)} = \frac{\partial\Gamma_{\alpha\beta}^{l(+)}}{\partial x^l} - \frac{\partial\Gamma_{\alpha l}^{l(+)}}{\partial x^\beta} + \Gamma_{\alpha\beta}^{l(+)}\Gamma_{lm}^{m(+)} - \Gamma_{\alpha l}^{m(+)}\Gamma_{m\beta}^{l(+)} \tag{77}$$

is the Ricci tensor of the outer side of the local section of the 2^3-$\lambda_{m,n}$-vacuum (i.e., the *subcont*);

$$R_{\alpha\beta}^{(-)} = \frac{\partial\Gamma_{\alpha\beta}^{l(-)}}{\partial x^l} - \frac{\partial\Gamma_{\alpha l}^{l(-)}}{\partial x^\beta} + \Gamma_{\alpha\beta}^{l(-)}\Gamma_{lm}^{m(-)} - \Gamma_{\alpha l}^{m(-)}\Gamma_{m\beta}^{l(-)} \tag{78}$$

is the Ricci tensor of the inner side of the local section of the 2^3-$\lambda_{m,n}$-vacuum (i.e., the antisubcont);

$$\Gamma_{\alpha\beta}^{\lambda(+)} = \frac{1}{2}g^{\lambda\mu(+)}\left(\frac{\partial g_{\mu\beta}^{(+)}}{\partial x^\alpha} + \frac{\partial g_{\alpha\mu}^{(+)}}{\partial x^\beta} - \frac{\partial g_{\alpha\beta}^{(+)}}{\partial x^\mu}\right) \tag{79}$$

are the Christoffel symbols of the local section of the *subcont*;

$$\Gamma_{\alpha\beta}^{\lambda(-)} = \frac{1}{2}g^{\lambda\mu(-)}\left(\frac{\partial g_{\mu\beta}^{(-)}}{\partial x^\alpha} + \frac{\partial g_{\alpha\mu}^{(-)}}{\partial x^\beta} - \frac{\partial g_{\alpha\beta}^{(-)}}{\partial x^\mu}\right) \tag{80}$$

are the Christoffel symbols of the *antisubcont*.

A feature of the geometrized vacuum physics developed here is to ensure the vacuum balance condition

$$S = \iiint \frac{1}{2}\left(R^{(+)} + R^{(-)}\right)dxdydz = 0, \tag{81}$$

it means that "convexity" and "concavity" (or compression and tension) over the entire 3-dimensional deformed region of the 2^3-$\lambda_{m,n}$-vacuum, on average, completely compensate each other (see Figure 14).

Preprints (www.preprints.org) | NOT PEER-REVIEWED | Posted: 5 October 2023 doi:10.20944/preprints202308.0570.v4

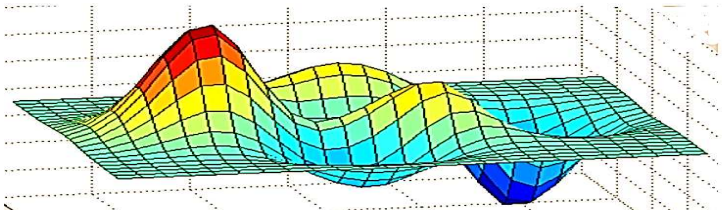

Figure 14. 2D-illustration of a convex-concave two-sided surface with stignatures {+ +} and {– +}. This curved surface is such that it is, on average, flat. At the same time, the deformation that looks like a convexity from the outside, from the inside it looks like a concavity. At the same time, it should be taken into account that if the stignatures of the sides of such a two-sided surface are completely opposite {+ +} and {– –}, then the deformations on its two sides are not only mutually opposite, but also mutually perpendicular (see §5.2).

So, in two-sided consideration, the non-zero components of the metric tensors (72) $g_{\alpha\beta}^{(+)}$ and $g_{\alpha\beta}^{(-)}$ are interconnected and describe the curvature of the 3-dimensional extension of the two-sided 2^3-$\lambda_{m,n}$-vacuum.

2.6.2. Zero components of the metric tensor

To clarify the physical meaning of the zero components of the metric tensors (32) and (35)

$$g_{i0}^{(+)} = \begin{pmatrix} g_{00}^{(+)} & g_{10}^{(+)} & g_{20}^{(+)} & g_{30}^{(+)} \\ g_{01}^{(+)} & \cdots & \cdots & \cdots \\ g_{02}^{(+)} & \cdots & \cdots & \cdots \\ g_{03}^{(+)} & \cdots & \cdots & \cdots \end{pmatrix}, \qquad g_{0j}^{(-)} = \begin{pmatrix} g_{00}^{(-)} & g_{10}^{(-)} & g_{20}^{(-)} & g_{30}^{(-)} \\ g_{01}^{(-)} & \cdots & \cdots & \cdots \\ g_{02}^{(-)} & \cdots & \cdots & \cdots \\ g_{03}^{(-)} & \cdots & \cdots & \cdots \end{pmatrix}, \tag{82}$$

let's use the kinematics of the layers of the two-sided 2^3-$\lambda_{m,n}$-vacuum.

Under the kinematics of vacuum layers is meant such a section of geometrized vacuum physics based on the Algebra of Signatures (Alsigna), in which the displacements (movements) of different sides of the $\lambda_{m,n}$-vacuum are considered independently of their deformations. With a more consistent approach, i.e. during the development of the dynamics of vacuum layers in subsequent articles of this cycle, it turns out that any displacement of the local region of one layer of $\lambda_{m,n}$-vacuum is inevitably accompanied by its curvature. This, in turn, sets in motion the curvature of other adjacent layers of the $\lambda_{m,n}$-vacuum. At the same time, and vice versa, the curvature of the local region of one layer of the $\lambda_{m,n}$-vacuum is necessarily accompanied by its displacement (i.e., flow), which leads to a disturbance of all adjacent layers. In what follows, interconnected flows and curvatures of local sections of different layers of the $\lambda_{m,n}$-vacuum are considered as multidimensional 4-deformations using the mathematical apparatus of the general theory of relativity.

Despite the above shortcomings, kinematic models of the motion of various layers of the 2^3-$\lambda_{m,n}$-vacuum make it possible to elucidate the physical meaning of the zero components of metric tensors and theoretically predict a number of previously unknown vacuum effects that can be tested in practice.

Let the initial (stationary and non-curved) state of the two-sided 2^3-$\lambda_{m,n}$-vacuum be given by a set of pseudo-Euclidean metrics (36a) and (51a)

$$\begin{cases} ds_0^{(+)2} = \; c^2dt^2 - dx^2 - dy^2 - dz^2 = ds^{(+)\prime}ds^{(+)\prime\prime} = \; cdt'cdt'' - dx'dx'' - dy'dy'' - dz'dz''; \\ ds_0^{(-)2} = -c^2dt^2 + dx^2 + dy^2 + dz^2 = ds^{(-)\prime}ds^{(-)\prime\prime} = -cdt'cdt'' + dx'dx'' + dy'dy'' + dz'dz'', \end{cases} \tag{83}$$

where the symbols are introduced

$$ds^{(+)\prime} = \; c\,dt' + idx' + jdy' + kdz' \quad \text{is mask of the } subcont; \tag{84}$$

Preprints (www.preprints.org) | NOT PEER-REVIEWED | Posted: 5 October 2023 doi:10.20944/preprints202308.0570.v4

$$ds^{(+)\prime\prime} = c\,dt'' + i dx'' + j dy'' + k dz'' \quad \text{is interior of the } subcont; \tag{85}$$

$$ds^{(-)\prime} = -c\,dt' + i dx' + j dy' + k dz' \quad \text{is mask of the } antisubcont; \tag{86}$$

$$ds^{(-)\prime\prime} = c\,dt'' - i dx'' - j dy'' - k dz'' \quad \text{is interior of the } antisubcont, \tag{87}$$

is affine aggregates, in particular, quaternions with a multiplication table of imaginary units, for example,

	i	j	k
i	-1	k	$-j$
j	$-k$	-1	i
k	j	$-i$	-1

(88)

We consider three kinematic cases:

1). In the first case, let the *mask* and the *interior* of the outer and inner sides of the 2^3-$\lambda_{m,n}$-vacuum move relative to the initial stationary state along the x axis with the same velocity v_x,, but in different directions. This is formally described by the transformation of coordinates [7]:

$$t' = t, \quad x' = x + v_x t, \quad y' = y, \quad z' = z \quad \text{– for the } mask; \tag{89}$$

$$t'' = t, \quad x'' = x - v_x t, \quad y'' = y, \quad z'' = z \quad \text{– for the } interior. \tag{90}$$

The equality of the modules of the speeds of movement v_x of the *mask* and the *interior* is due to the condition of 2^3-$\lambda_{m,n}$-vacuum balance, which requires that each movement in the 2^3-$\lambda_{m,n}$-vacuum corresponds to a similar anti-motion.

We differentiate expressions (89) and (90) taking into account that x' is a function of two variables $x'(x,t)$ and v_x = const, and substitute the results of differentiation into metrics (83), as a result we obtain a set of metrics

$$\begin{cases} ds^{(+)2} = \left(1 + \dfrac{v_x^2}{c^2}\right) c^2 dt^2 - dx^2 - dy^2 - dz^2, \\ ds^{(-)2} = -\left(1 + \dfrac{v_x^2}{c^2}\right) c^2 dt^2 + dx^2 + dy^2 + dz^2, \end{cases} \tag{91}$$

which describe the kinematics of the joint motion of the outer side of the 2^3-$\lambda_{m,n}$-vacuum (i.e. *subcont*) and its inner side (*antisubcont*), subject to the vacuum balance condition

$$ds^{(-)2} + ds^{(+)2} = 0. \tag{92}$$

The zero components of the metric tensors (82) in this case are equal to

$$g_{0j}^{(+)} = \begin{pmatrix} 1 + v_x^2/c^2 & 0 & 0 & 0 \\ 0 & \dots & \dots & \dots \\ 0 & \dots & \dots & \dots \\ 0 & \dots & \dots & \dots \end{pmatrix}, \qquad g_{i0}^{(-)} = \begin{pmatrix} -1 - v_x^2/c^2 & 0 & 0 & 0 \\ 0 & \dots & \dots & \dots \\ 0 & \dots & \dots & \dots \\ 0 & \dots & \dots & \dots \end{pmatrix}. \tag{93}$$

the *mask* and the *interior* of the outer and inner sides of the 2^3-$\lambda_{m,n}$-vacuum.

2). In the second case, let the *mask* and the *interior* of the outer and inner sides of the 2^3-$\lambda_{m,n}$-vacuum (i.e., of the *subcont* and *antisubcont*) move relative to their initial stationary state in the same direction - along the x axis with the same speed v_x. This is formally described by the coordinate transformations:

$$t' = t, \quad x' = x - v_x t, \quad y' = y, \quad z' = z \quad \text{– for the } mask; \tag{94}$$

$$t'' = t, \quad x'' = x - v_x t, \quad y'' = y, \quad z'' = z \quad \text{– for the } interior. \tag{95}$$

We differentiate Exs. (94) and (95) taking into account that x' is a function of two variables $x'(x,t)$ and v_x = const, and substitute the results of differentiation into metrics (83), as a result we obtain a set of metrics

Preprints (www.preprints.org) | NOT PEER-REVIEWED | Posted: 5 October 2023 doi:10.20944/preprints202308.0570.v4

$$\begin{cases} ds^{(+)2} = \left(1-\dfrac{v_x^2}{c^2}\right)c^2dt^2 + v_xdxdt + v_xdtdx - dx^2 - dy^2 - dz^2, \\ ds^{(-)2} = -\left(1-\dfrac{v_x^2}{c^2}\right)c^2dt^2 - v_xdxdt - v_xdtdx + dx^2 + dy^2 + dz^2. \end{cases} \quad (96)$$

In this case, 2^3-$\lambda_{m,n}$-vacuum balance is also observed, because $ds^{(-)2} + ds^{(+)2} = 0$, but additional cross terms v_xdxdt are appear. In this case, the zero components of the metric tensors (82) are equal to

$$g_{0j}^{(+)} = \begin{pmatrix} 1-v_x^2/c^2 & v_x & 0 & 0 \\ v_x & \dots & \dots & \dots \\ 0 & \dots & \dots & \dots \\ 0 & \dots & \dots & \dots \end{pmatrix}, \quad g_{i0}^{(-)} = \begin{pmatrix} -1+v_x^2/c^2 & -v_x & 0 & 0 \\ -v_x & \dots & \dots & \dots \\ 0 & \dots & \dots & \dots \\ 0 & \dots & \dots & \dots \end{pmatrix}. \quad (97)$$

3) In the third case, let the *mask* and the *interior* of the outer and inner sides of the 2^3-$\lambda_{m,n}$-vacuum (i.e., of the *subcont* and *antisubcont*) rotate around the z-axis in the same direction with the angular velocity Ω. These processes are described by the coordinate transformations [7]:

$$\begin{aligned} t' &= t, \quad x' = x\cos\Omega t - y\sin\Omega t, \quad z' = z, \quad y' = x\sin\Omega t + y\cos\Omega t, \\ t'' &= t, \quad x'' = x\cos\Omega t - y\sin\Omega t, \quad z'' = z, \quad y'' = x\sin\Omega t + y\cos\Omega t. \end{aligned} \quad (98)$$

We differentiate Exs. (89) and substitute the results of differentiation into metrics (83), as a result we obtain the metrics [7]

$$\begin{cases} ds^{(+)2} = \left[1-\dfrac{\Omega^2}{c^2}(x^2+y^2)\right]c^2dt^2 + 2\Omega ydxdt - 2\Omega xdydt - dx^2 - dx^2 - dz^2, \\ ds^{(-)2} = -\left[1-\dfrac{\Omega^2}{c^2}(x^2+y^2)\right]c^2dt^2 - 2\Omega ydxdt + 2\Omega xdydt + dx^2 + dx^2 + dz^2. \end{cases} \quad (99)$$

In this case, the 2^3-$\lambda_{m,n}$-vacuum balance $ds^{(+)2} + ds^{(-)2} = 0$ is observed, and the zero components of the metric tensors (82) are equal to

$$g_{0j}^{(+)} = \begin{pmatrix} 1-\frac{\Omega^2}{c^2}(x^2+y^2) & 2\Omega y & 0 & 0 \\ -2\Omega x & \dots & \dots & \dots \\ 0 & \dots & \dots & \dots \\ 0 & \dots & \dots & \dots \end{pmatrix}, \quad g_{0i}^{(-)} = \begin{pmatrix} -1+\frac{\Omega^2}{c^2}(x^2+y^2) & -2\Omega y & 0 & 0 \\ 2\Omega x & \dots & \dots & \dots \\ 0 & \dots & \dots & \dots \\ 0 & \dots & \dots & \dots \end{pmatrix}. \quad (100)$$

It can be seen from the considered kinematic examples that the zero components of the metric tensors (82) are associated not with deformations, but with the translational and/or rotational motion of various layers of the 2^3-$\lambda_{m,n}$-vacuum.

2.7. Predictions of the kinetics of vacuum layers

2.7.1. The limiting speed of movement of 2^3-$\lambda_{m,n}$-vacuum layers

Let's consider one of the metrics (96)

$$ds^{(+)2} = (1-v_x^2/c^2)c^2dt^2 + 2v_xdxdt - dx^2 - dy^2 - dz^2. \quad (101)$$

We single out in the metric (101) the full square [7,8]

$$ds^{(-)2} = dt^2\left[c\sqrt{1-\frac{v_x^2}{c^2}} - \frac{v_x}{cdt}\frac{dx}{\sqrt{1-\frac{v_x^2}{c^2}}}\right]^2 - \frac{dx^2}{1-\frac{v_x^2}{c^2}} - dy^2 - dz^2, \quad (102)$$

and introduce the notation

$$c' = c\sqrt{1-\frac{v_x^2}{c^2}} - \frac{v_x}{cdt}\frac{x}{\sqrt{1-\frac{v_x^2}{c^2}}}, \quad t' = t, \quad x' = \frac{x}{\sqrt{1-\frac{v_x^2}{c^2}}}, \quad y' = y, \quad z' = z. \quad (103)$$

In these notations, metric (102) takes the form [7]

Preprints (www.preprints.org) | NOT PEER-REVIEWED | Posted: 5 October 2023 doi:10.20944/preprints202308.0570.v4

$$ds^{(-)^2} = c'^2dt'^2 - dx'^2 - dy'^2 - dz'^2, \quad (104)$$

corresponding to the propagation of a beam of light in the reference system of the observer, which moves together with the moving side of the 2^3-$\lambda_{m,n}$-vacuum.

In this case, the metric (102) describes the propagation of a light beam in a layer of vacuum, which moves with a constant speed v_x relative to the reference system of a stationary observer. This is similar to how a stationary observer measures the speed of waves propagating along a moving surface of water (for example, a river). Such an observer will find that the speed of propagation of wave disturbances depends on the speed of the river flow, while relative to the water itself, the speed of wave propagation remains unchanged, and depends only on the properties of the water itself (its density, temperature, impurities, etc.).

From the first Ex. (103)

$$c' = c\sqrt{1-\frac{v_x^2}{c^2}} - \frac{v_x}{cdt}\frac{x}{\sqrt{1-\frac{v_x^2}{c^2}}}. \quad (105)$$

it can be seen that in the case of (94) – (96) the speed v_x of the outer side of the 2^3-$\lambda_{m,n}$-vacuum (*subcont*) and its inner side (*antisubcontact*) cannot exceed the speed of light c (the velocity of propagation of wave disturbances along these sides), i.e. $v_x < c$.

However, for the case (89) – (91) the situation is different. Let's consider this variant of intravacuum processes using the example of *subcont* movement described by the metric (91)

$$ds^{(-)2} = (1+ v_x^2/c^2)c^2dt^2 - dx^2 - dy^2 - dz^2. \quad (106)$$

In this case, the introduction of the notation

$$c' = c\sqrt{1+\frac{v_x^2}{c^2}}, \quad t' = t, \quad x' = x, \quad y' = y, \quad z' = z. \quad (107)$$

reduces the metric (106) to the form (104). At the same time, it can be seen from Exs. (107) that there are no restrictions on the speeds v_x of the *mask* and the *interior* of the *subcont*. This circumstance requires a separate detailed consideration, since it allows the possibility of organizing superluminal intra-vacuum communication channels by controlling the movement of vacuum layers. This is one of the possible theoretical predictions of the kinetics of the 2^3-$\lambda_{m,n}$-vacuum layers.

2.7.2. Inert properties of layers of 2^3-$\lambda_{m,n}$-vacuum

Let's return to the consideration of metrics (83)

$$ds^{(+---)2} = ds^{(+)2} = c^2dt^2 - dx^2 - dy^2 - dz^2, \quad (108)$$

$$ds^{(-+++)2} = ds^{(-)2} = -c^2dt^2 + dx^2 + dy^2 + dz^2. \quad (109)$$

Let us take out the value c^2dt^2 on the right-hand sides of these metrics [7]

$$ds^{(+)^2} = c^2dt^2(1-\frac{v^2}{c^2}), \quad (110)$$

$$ds^{(-)^2} = -c^2dt^2(1-\frac{v^2}{c^2}), \quad (111)$$

where $v = (dx^2+dy^2+dz^2)^{1/2}/dt = dl/dt$ is the 3-dimensional velocity.

We extract the root of the two sides of Exs. (110) and (111). As a result, according to the symbols (84) – (87), we get

$$ds^{(+)'} = cdt\sqrt{1-\frac{v^2}{c^2}} \quad \text{– for mask of the } subcont; \quad (112)$$

Preprints (www.preprints.org) | NOT PEER-REVIEWED | Posted: 5 October 2023 doi:10.20944/preprints202308.0570.v4

$$ds^{(+)''} = -cdt\sqrt{1-\frac{v^2}{c^2}} \quad \text{– for interior of the } subcont; \tag{113}$$

$$ds^{(-)'} = icdt\sqrt{1-\frac{v^2}{c^2}} \quad \text{– for mask of the } antisubcont; \tag{114}$$

$$ds^{(-)'} = -icdt\sqrt{1-\frac{v^2}{c^2}} \quad \text{– for interior of the } antisubcont. \tag{115}$$

For example, consider the 4-dimensional velocity vector of the mask of the *subcont*

$$u_i{}^{(+)} = dx^i/ds^{(+)'}. \tag{116}$$

We substitute the linear form (112) into Ex. (116), as a result, we obtain the components of the 4-velocity of the mask of the *subcont* [7,8]

$$u_i^{(+)} = \left[\frac{1}{\sqrt{1-\frac{v^2}{c^2}}}, \frac{v_x}{c\sqrt{1-\frac{v^2}{c^2}}}, \frac{v_y}{c\sqrt{1-\frac{v^2}{c^2}}}, \frac{v_z}{c\sqrt{1-\frac{v^2}{c^2}}}\right]. \tag{117}$$

Let the mask of the *subcont* move only in the direction of the x-axis, then its 4-velocity has components

$$u_i^{(-)} = \left[\frac{1}{\sqrt{1-\frac{v_x^2}{c^2}}}, \frac{v_x}{c\sqrt{1-\frac{v_x^2}{c^2}}}, 0, 0\right]. \tag{118}$$

Let's now define the 4-acceleration of the mask of the *subcont* [8]

$$\frac{du_i^{(+)}}{cdt} = \left[\frac{d}{cdt}\left(\frac{1}{\sqrt{1-\frac{v_x^2}{c^2}}}\right), \frac{d}{cdt}\left(\frac{v_x}{c\sqrt{1-\frac{v_x^2}{c^2}}}\right), 0, 0\right] \tag{119}$$

and to simplify, consider only its x-component 4-velocity

$$\frac{du_x^{(+)}}{cdt} = \frac{d}{cdt}\left(\frac{v_x}{c\sqrt{1-\frac{v_x^2}{c^2}}}\right), \tag{120}$$

where the value

$$\frac{d}{dt}\left(\frac{v_x}{\sqrt{1-\frac{v_x^2}{c^2}}}\right) = a_x^{(+)} \tag{121}$$

has the dimension of the x-component of the 3-dimensional acceleration of the local section of the mask of the *subcont*.

On the left side of Ex. (121), we perform the differentiation operation [8]

$$a_x^{(+)} = \left(\frac{1}{\sqrt{1-\frac{v_x^2}{c^2}}} + \frac{v_x^2}{c^2\left(1-\frac{v_x^2}{c^2}\right)^{\frac{3}{2}}}\right)\frac{dv_x}{dt}, \tag{122}$$

and introduce the notation

$$dv_x/dt = a_x{}^{(+)'}. \tag{123}$$

In this case, Ex. (122) takes the form

Preprints (www.preprints.org) | NOT PEER-REVIEWED | Posted: 5 October 2023 doi:10.20944/preprints202308.0570.v4

$$a_x^{(+)} = \left(\frac{1}{\sqrt{1-\frac{v_x^2}{c^2}}} + \frac{v_x^2}{c^2\left(1-\frac{v_x^2}{c^2}\right)^{\frac{3}{2}}} \right) a_x^{(+)\prime}, \tag{124}$$

where

$a_x^{(+)}$ is the actual acceleration section of the mask of the *subcont*, taking into account its inert properties; $a_x^{(+)\prime}$ is the ideal acceleration of the same section of the mask of the *subcont*, without taking into account its inert properties.

Let's represent Ex. (124) in the following form

$$a_x^{(+)} = \mu_x^{(+)} a_x^{(+)\prime}, \tag{125}$$

where

$$\mu_x^{(+)} = \left(\frac{1}{\sqrt{1-\frac{v_x^2}{c^2}}} + \frac{v_x^2}{c^2\left(1-\frac{v_x^2}{c^2}\right)^{\frac{3}{2}}} \right) \tag{126}$$

is the dimensionless kinematic coefficient of inertia of the local area of the mask of the *subcont*, which relates the actual and ideal accelerations of this 2^3-$\lambda_{m,n}$-vacuum layer. This coefficient shows, within the framework of the kinematic approach, how the inertness (i.e., resistance to a change in the state of movement) of this section of the mask of the *subcont* changes with a change in the speed of its movement.

It follows from Ex. (126) that at $v_x = 0$ the kinematic inertia coefficient $\mu_x^{(+)} = 1$ and $a_x^{(+)} = a_x^{(+)\prime}$. This means that the section of the mask of the *subcont* does not exert any resistance to the beginning of its movement (or displacement). As v_x approaches the speed of light c, the kinematic inertia coefficient $\mu_x^{(+)}$ tends to infinity, while further acceleration of this 2^3-$\lambda_{m,n}$-vacuum layer becomes impossible.

Ex. (126) is a massless analog of Newton's second law

$$F_x = ma_x', \tag{127}$$

where F_x is the x-component of the force vector; m is body weight; a_x' is the x-component of its ideal acceleration.

Comparing Exs. (125) and (127), we find that the dimensionless coefficient of inertia $\mu_x^{(-)}$ of the local area of the mask of the *subcont* is a dimensionless analogue of the density of the inertial mass of a continuous medium.

Sequentially performing actions (116) – (126) with metrics (113) – (115), we obtain the kinematic inertia coefficients $\mu_x^{(+)\prime\prime}$, $\mu_x^{(-)\prime}$, $\mu_x^{(-)\prime\prime}$ for three the remaining layers of the two-sided 2^3-$\lambda_{m,n}$-vacuum. The overall kinetic inertia coefficient of the local two-sided section of the 2^3-$\lambda_{m,n}$-vacuum is a function of all four inertia coefficients

$$\mu_x^{(\pm)} = f\left(\mu_x^{(+)\prime}, \mu_x^{(-)\prime\prime}, \mu_x^{(-)\prime}, \mu_x^{(-)\prime\prime}\right). \tag{128}$$

The explicit form of this function is determined when describing the dynamics of 2^3-$\lambda_{m,n}$-vacuum, which will be presented in subsequent articles of this project.

2.7.3. *Kinematics of the rupture of the local section of the 2^3-$\lambda_{m,n}$-vacuum*

"For in much wisdom is much vexation, and he
who increases knowledge increases sorrow."
Kohelet (Ecclesiastes 1:18)

Let's consider the kinematic aspects of the possibility of a "rupture" of the of the local section of the two-sided 2^3-$\lambda_{m,n}$-vacuum.

We integrate Ex. (121) [8]

Preprints (www.preprints.org) | NOT PEER-REVIEWED | Posted: 5 October 2023 doi:10.20944/preprints202308.0570.v4

$$\frac{v_x}{\sqrt{1-\frac{v_x^2}{c^2}}} = a_x t + const. \tag{129}$$

Integrating expression (129) once more and setting $x_0 = 0$ at $t = 0$, we obtain the following change in the length of the mask of the *subcont* of the 2^3-$\lambda_{m,n}$-vacuum along the x axis during its accelerated motion [8]:

$$x - x_0 = \Delta x = \frac{c^2}{a_x}\left(\sqrt{1+\frac{a_x^2 t^2}{c^2}} - 1\right). \tag{130}$$

Let the initial (i.e., immobile) state of the local section of the *subcont* be given by the metric (108)

$$ds^{(-)^2} = c^2 dt'^2 - dx'^2 - dy'^2 - dz'^2 . \tag{131}$$

The uniformly accelerated motion of this section along the x axis is formally specified by the coordinate transformation [8]:

$$t' = t, \quad x' = x + \Delta x = x + \frac{c^2}{a_x}\left(\sqrt{1+\frac{a_x{}^2 t^2}{c^2}} - 1\right), \quad y' = y, \quad z' = z. \tag{132}$$

Differentiating the coordinates (132) and substituting the results of differentiation into the metric (131), we obtain the following metric [8]

$$ds_a^{(+)2} = \frac{c^2 dt^2}{1+\frac{a_x{}^2 t^2}{c^2}} - \frac{2a_x t dt dx}{\sqrt{1+\frac{a_x{}^2 t^2}{c^2}}} - dx^2 - dy^2 - dz^2, \tag{133}$$

which describes the uniformly accelerated motion of the local section of the *subcont* (i.e., the outer side of the 2^3-$\lambda_{m,n}$-vacuum) in the direction of the x axis.

If, in the same area of the *subcont*, an additional flow with uniformly slow motion (i.e., with negative acceleration) is created,

$$\frac{d}{dt}\left(\frac{v_x}{\sqrt{1-\frac{v_x^2}{c^2}}}\right) = -a_x \tag{134}$$

then, doing mathematical calculations similar to (130) – (133), we get the metric

$$ds_b^{(+)2} = \frac{c^2 dt^2}{1-\frac{a_x^2 t^2}{c^2}} - \frac{2a_x t dt dx}{\sqrt{1-\frac{a_x^2 t^2}{c^2}}} - dx^2 - dy^2 - dz^2. \tag{135}$$

In this case, the average metric-dynamic state of the local section of the *subcont* will be characterized by the averaged metric

$$< ds^{(+)} >^2 = \frac{1}{2}\left(ds_a^{(+)2} + ds_b^{(+)2}\right) = \frac{c^2 dt^2}{1-\frac{a_x^4 t^4}{c^4}} - \frac{a_x t\left(\sqrt{1-\frac{a_x^2 t^2}{c^2}} + \sqrt{1+\frac{a_x^2 t^2}{c^2}}\right) dt dx}{\sqrt{1-\frac{a_x^4 t^4}{c^4}}} - dx^2 - dy^2 - dz^2$$

with signature (+ – – –). (136)

It can be seen from the metric (106) that in the case

$$\frac{a_x^4 t^4}{c^4} = 1, \quad \text{or} \quad |a_x| t = c \quad \text{or} \quad |a_x| = c/\Delta t, \tag{137}$$

Preprints (www.preprints.org) | NOT PEER-REVIEWED | Posted: 5 October 2023 doi:10.20944/preprints202308.0570.v4

the first and second terms in the averaged metric (136) go to infinity. This singularity can be interpreted as a "rupture" of the *subcont* area under study (i.e., a "rupture" of the local region of the 2^3-$\lambda_{m,n}$-vacuum outer side).

Breaking a *subcont* is an incomplete action. For a complete "rupture" of the local section of the 2^3-$\lambda_{m,n}$-vacuum, it is necessary to "break" its inner side, described by the metric (109) with the signature (– + + +). To do this, it is necessary to create similar uniformly accelerated and uniformly retarded flows in the same region of space in the *antisubcont* (i.e., in the inner side of the 2^3-$\lambda_{m,n}$-vacuum), so that its average state is determined by the averaged metric

$$< ds^{(-)} >^2 = \frac{1}{2}\left(ds_a^{(-)2} + ds_b^{(-)2}\right) = -\frac{c^2dt^2}{1-\frac{a_x^4t^4}{c^4}} + \frac{a_xt\left(\sqrt{1-\frac{a_x^2t^2}{c^2}}+\sqrt{1+\frac{a_x^2t^2}{c^2}}\right)dtdx}{\sqrt{1-\frac{a_x^4t^4}{c^4}}} + dx^2 + dy^2 + dz^2, \quad (138)$$

with a signature (– + + +), which "breaks" under the same conditions

$$\frac{a_x^4t^4}{c^4} = 1, \text{ or } \quad |a_x|t = c, \quad \text{or} \quad |a_x| = c/\Delta t. \quad (139)$$

Averaging metrics (136) and (138) leads to the fulfillment of the vacuum condition

$$<< ds >>^2 = {}^1/_2\,(< ds^{(+)} >^2 + < ds^{(-)} >^2) = 0 \quad (140)$$

which in this situation is equivalent to Newton's third law: – "Action is equal to reaction":

$$F_x^{(+)} - F_x^{(-)} = ma_x^{(+)} - ma_x^{(-)} = a_x^{(+)} - a_x^{(-)}. \quad (141)$$

That is, the process of "rupture" of the local region of the $\lambda_{m,n}$-vacuum is similar to the rupture of an ordinary (atomistic) solid body, to which sufficiently large equal forces (more precisely, accelerations) are applied from its two sides.

It is not excluded that the conditions of "rupture" described above $\lambda_{-11,-13}$-vacuum are formed in the collision of oncoming flows of elementary particles accelerated on the collider. It is possible that a strong collision of particles leads to the emergence of a web of vacuum "cracks", while the closed cracks scatter in the form of many new "particles" and "antiparticles".

To obtain "rupture" of the vacuum of large scales, it is necessary to initiate accelerated flows of different sides of the $\lambda_{2,3}$-vacuum (see §1 in the article [1]).

Apparently, "ruptures" of vacuum of various scales occur in the nature around us, for example, when new particles are born from the void during the collision of atmospheric molecules with cosmic radiation, or during lightning flashes in rain clouds. We are here only trying to describe these phenomena on the basis of a geometrized vacuum physics based on the Algebra of Signatures. However, the development of "zero" (vacuum) technologies is fraught with great dangers. Therefore, in parallel with the development of vacuum physics (in particular, the kinetics of vacuum layers), it is necessary to rethink the religious and philosophical aspects of modern science, to develop "Vacuum Ethics", "Vacuum Aesthetics" and "Vacuum Psychology". Otherwise, this knowledge will not benefit our civilization [5,9].

3. Conclusions

"Whoever fights monsters, you yourself do not become a monster. And when you gaze long into an Abyss, the Abyss also gazes into you."

Friedrich W. Nietzsche

"Jenseits Gut und böse" (Beyond Good and evil)

This article is the third part of a unified study under the general title "Geometrized vacuum physics based on the Algebra of Signatures".

In the first two parts of this study, presented in the author's articles [1,2], a method was proposed for studying an ideal (i.e., non-curved and stationary) vacuum region by probing it with mutually perpendicular light rays with different wavelengths $\lambda_{m,n}$. This method made it possible in the first

two articles [1,2] to lay the foundations first of the Algebra of Stignatures, and then of the Algebra of Signatures.

This article considers the possibilities of describing the curved state of the same region of the vacuum on the basis of further development of the mathematical apparatus of the Algebra of Signatures.

We list the main results obtained in this article:

1) On the example of one of the $\lambda_{m,n}$-vacuums, it is shown that many levels of consideration of its curvatures are possible. The simplest of them is at least double-sided. This level of consideration implies that the empty space (vacuum) surrounding us has at least two 4-dimensional sides, which can be conditionally called: the outer side with the Minkowski space signature (+ − − −), and the inner side with the completely opposite signature of anti-Minkowski space (− + + +). In this case, to describe the curvature of the local region of the two-sided 2^3-$\lambda_{m,n}$-vacuum, not 16 components of the metric tensor are required, as in a one-sided theory, for example, in general relativity, but 16 + 16 = 32 = 2^5 components of the metric tensor. The next level of consideration is the $\lambda_{m,n}$-vacuum with 16 sides. At this level of consideration, to describe the curvature of the local region of the sixteen-sided 2^6-$\lambda_{m,n}$-vacuum, already 16 × 16 = 256 = 2^8 components of the metric tensor are required. In this case, the description of the curvature is much more accurate than with a two-sided description. The mathematical apparatus of the Algebra of Stignatures provides for the possibility of increasing the number of metric tensor components describing the curvature of the local region of the $\lambda_{m,n}$-vacuum to infinity (see §2.9 in [2]).

2) It is shown that a length element on one side of a two-sided space with completely opposite signatures corresponds to a perpendicular element on its other side (see §2.5.2 of this article). This, at first glance, simple observation entails very significant consequences. This circumstance is the reason why many intra-vacuum and macroscopic processes turn into spirals.

3) The physical meaning of the zero and non-zero components of the metric tensor is revealed in the framework of the proposed "Geometrized vacuum physics" (see §2.6 of this article).

4) The 4-strain tensor and the components of the relative elongation vector are introduced for two-sided and 16-sided consideration of the $\lambda_{m,n}$-vacuum curvatures (see §§2.5.2 and 2.5.3 of this article).

5) Some aspects of the kinematics of the layers of $\lambda_{m,n}$-vacuum are considered (see §2.7 of this article). This made it possible to analyze the inert properties of the $\lambda_{m,n}$-vacuum (see §2.7.1), and to predict the possibility of displacement of vacuum layers at a speed much higher than the speed of light (see §2.7.2). At the same time, it is shown that the longitudinal displacement of the outer and inner sides of the $\lambda_{m,n}$-vacuum relative to each other inevitably leads to their twisting into a spiral bundle.

6) A kinematic model of the possibility of a local “rupture” of $\lambda_{m,n}$-vacuum is considered (see §2.7.3).

The "Geometrized vacuum physics based on the Algebra of Signatures" proposed in articles [1,2] and in this article is far from being completed, but already now, within the framework of this research program, the possibility of developing “zero” (i.e., vacuum) technologies. At the same time, it is obvious that the development of these technologies requires a significant increase in the responsibility of mankind to the Universe [5,9].

Acknowledgments: I express my sincere gratitude to R. Gavriil Davydov, David Reid and R. Eliezer Rahman for their assistance. The discussion of the article was attended by Academician of the Russian Academy of Sciences Shipov G.I., Ph.D. Lukyanov V.A., Lebedev V.A., Prokhorov S.G. and Khramikhin V.P. Also, the author is grateful for the support of Salova M.N., Morozova T.S., Przhigodsky S.V., Maslov A.N., Bolotov A.Yu., Ph.D. Levi T.S., Musanov S.V., Batanova L.A., Ph.D. Myshelov E.P., Chivikov E.P.

References

1. Batanov-Gaukhman, M. (2023) “Geometrized vacuum physics. Part I. Algebra of Stignatures“. https://doi.org/10.20944/preprints202306.0765.v1.

2. Batanov-Gaukhman, M. (2023) “Geometrized vacuum physics. Part II. Algebra of Signatures“. https://doi.org/10.20944/preprints202307.0716.v1.
3. Sedov, L.I. (1994) ”Continuum mechanics. T1”, – Moscow: Nauka, [in Russian]. (Available in English "A course in continuum mechanics", translation from the Russian, ed. by J. R. M. Radok).
4. Shipov, G. (1998) ”A Theory of Physical Vacuum”, – Moscow ST-Center, Russia ISBN 5 7273-0011-8. (available in English).
5. Gaukhman, M.Kh. (2007) "Algebra of Signatures "Void" (yellow Alsigna), – Moscow: URSS, p. 308, ISBN 978-5-382-00580-5, (available at www.alsigna.ru).
6. Gaukhman, M.Kh. (2017) "Algebra of Signatures "Massless physics" (purple Alsigna). – Moscow: Filin, ISBN 978-5-9216-0104-8 (available in English http://metraphysics.ru/).
7. Landau, L.D. & Lifshits, E.M. (1988) "Field theory". Vol. 2. – Moscow: Nauka, p. 509, ISBN 5-02-014420-7 [in Russian]. (available in English "The Classical theory of fields", Vol. 2. fourth English edition).
8. Logunov, A.A. (1987) "Lectures on the theory of relativity and gravity", – Moscow: Nauka, p. 271 [in Russian].
9. Gaukhman, M.Kh. (2007) "Algebra of Signatures "NAMES" (orange Alsigna), – Moscow: LKI, p.228, ISBN 978-5-382-00077-0 (available on site www.alsigna.ru) [in Russian].